

Non-Intrusive Predictive Health Monitoring for Wind Turbine Generators
Feasibility Study
Final Report

Prepared for

THE NEW YORK STATE
ENERGY RESEARCH AND DEVELOPMENT AUTHORITY
Albany, NY

Barry N. Liebowitz
Project Manager

Prepared by

MECHANICAL SOLUTIONS, INC.
Albany, NY

Thomas J. Walter
Project Manager

Agreement Number 18800

NYSERDA
Report Number xxx

September 2012

NOTICE

This report was prepared by Mechanical Solutions in the course of performing work contracted for and sponsored by the New York State Energy Research and Development Authority (hereafter "NYSERDA"). The opinions expressed in this report do not necessarily reflect those of NYSEDA or the State of New York, and reference to any specific product, service, process, or method does not constitute an implied or expressed recommendation or endorsement of it. Further, NYSEDA, the State of New York, and the contractor make no warranties or representations, expressed or implied, as to the fitness for particular purpose or merchantability of any product, apparatus, or service, or the usefulness, completeness, or accuracy of any processes, methods, or other information contained, described, disclosed, or referred to in this report. NYSEDA, the State of New York, and the contractor make no representation that the use of any product, apparatus, process, method, or other information will not infringe privately owned rights and will assume no liability for any loss, injury, or damage resulting from, or occurring in connection with, the use of information contained, described, disclosed, or referred to in this report.

ABSTRACT

Access to the nacelle of wind turbine generators to assess machinery running condition is a significant and universal problem. In the United States, modern condition based maintenance (CBM) data acquisition and communications hardware may not even be allowed to be installed in the nacelle, depending on warranty and other business arrangements between the owner, operator, and wind turbine manufacturer. As wind turbine warranties end, the problem of economically monitoring machinery health and maintaining turbine availability falls to the owner/operator.

Work accomplished under this NYSERDA project has, based on site and lab tests, established the feasibility of using non-intrusive advanced vibration-based diagnostic/prognostic methodology. The innovation is that all measurements are taken at the base of the tower – access to the nacelle or sensors mounted on the gearbox and generator are not required. As related herein, a portable, easy-to-use data acquisition and processing system has been established and a prototype has been used to acquire and effectively process lab and field data. Initial use by and feedback from potential users has been positive.

Implementing this technology can effectively increase the availability of wind turbines, reduce greenhouse gases, and use/advance the technology and industrial base in New York State.

KEY WORDS

Wind Turbines, Operation and Maintenance, Condition Based Maintenance, Predictive Maintenance, Vibration Monitoring, Machinery Diagnostics.

ACKNOWLEDGEMENTS

On several occasions, staff at Noble Environmental Power Company's North Country – New York windpark afforded access to multiple wind turbines for data collection and assessment of acquisition and processing methods. In this regard, Noble provided staff assistance to enable safe field operations and the opportunity to collect vibration and other data needed to establish and verify the techniques implemented. Noble also provided valuable feedback on the usability of the prototype system developed in this project.

During the initial and final stages of the project, site staff at the EDP-R Maple Ridge wind farm in Lowville, NY and the EGP/ENEL Green Power Fenner plant in Cazenovia, NY hosted visits by Mechanical Solutions, Inc. (MSI) personnel to introduce and summarize the project, and provided important feedback regarding the work planned and accomplished.

TABLE OF CONTENTS

<u>Section</u>	<u>Page</u>
ABSTRACT AND KEY WORDS	iii
ACKNOWLEDGEMENTS	iv
FIGURES	vi
TERMS	vii
SUMMARY	S-1
1 INTRODUCTION.....	1-1
2 IN-HOUSE TESTS	2-1
Test Rig	2-1
Test Data	2-3
Gearbox Modifications.....	2-3
3 WIND TURBINE VIBRATION DATA.....	3-1
May 2011	3-1
February 2012	3-2
4 TOWER ANALYSIS	4-1
Initial Model.....	4-1
Subsequent Model.....	4-2
5 PROTOTYPE DIAGNOSTIC SYSTEM.....	5-1
Signal Processing	5-1
Software	5-5
Hardware.....	5-11
Status and Future Work.....	5-13
6 TECHNOLOGY TRANSFER	6-1
2011 Wind Turbine Condition Monitoring Workshop.....	6-1
2012 AWEA Windpower Conference & Exhibition	6-2
Interaction with Wind Farm Operators	6-3
Interaction with Wind Turbine Manufacturer	6-4
Interaction with AWS Truepower	6-5
Interaction with AWEA	6-5
7 CONCLUSION, RECOMMENDATIONS and FUTURE WORK	7-1
Conclusions	7-1
Recommendations	7-1
On-Going and Planned Work.....	7-2
APPENDIX A: REPORT 1 FROM DR. RANDALL	A-1
APPENDIX B: REPORT 2 FROM DR. RANDALL.....	B-1
APPENDIX C: POSTER AT AWEA WINDPOWER 2012.....	C-1

FIGURES

<u>Figure</u>	<u>Page</u>
S-1	MSI Wind Farm Pro™ Prototype System..... S-2
2-1	Gearbox Test Rig at MSI. 2-1
2-2	Wind Turbine Tower Simulation Tube Added to Test Rig 2-2
2-3	In-House Test Rig as Finally Configured..... 2-3
2-4	Test Rig Typical Vibration Data 2-4
2-5	Tooth Fault Installed in One Tooth 2-5
2-6	Bearing Fault Installed in Outer Race 2-5
3-1	Comparison of Up-Tower and Down-Tower Vibration 3-1
3-2	Vibration Spectrum of Airborne Sound during Wind Turbine Operation..... 3-2
3-3	Comparison of Overall Down-Tower Vibration and Electric Power for Six Turbines 3-3
3-4	Turbine C-16 - Typical Vibration Overall Amplitude vs. Time Waveform..... 3-3
3-5	Turbine E-49 - Comparison of Power, Wind Speed, Generator Speed and Turbine Speed for 16+ hours..... 3-4
3-6	Turbine E-49 - Correlation of Overall Vibration at Tower Base vs. Turbine Power 3-5
3-7	Turbine E-49 - Comparison of Tower Base Acceleration vs. Turbine Power 3-5
3-8	Turbine E-49 - Comparison of Up- and Down-Tower Vibration..... 3-6
3-9	Turbine E-49 - Comparison of Acoustic and Down-Tower Vibration Data 3-6
3-10	Turbine E-49 - Acoustic Measurement Set-up Using a Parabolic Reflector 3-7
4-1	Initial (simplified) Finite Element Model of a Wind Turbine Tower..... 4-1
4-2	Subsequent (detailed) Finite Element Model of a Wind Turbine and Tower..... 4-2
5-1	Comparison of a Typical FFT Spectrum and a CPB Spectrum for the Same Data 5-4
5-2	Adding a Turbine to the Setup 5-6
5-3	Preparing to Record a Baseline 5-7
5-4	Recording a Baseline..... 5-7
5-5	Recording a Measurement..... 5-8
5-6	Trending Turbine Health..... 5-9
5-7	Advanced Bearing Diagnostics5-10
5-8	FFT of Amplitude Demodulated Data for a Healthy and Damaged Bearing5-12

TERMS

The following terms are described here to assist the interested reader who may not be familiar with some of the technical matter contained herein. These explanations are provided within the context used in this report and are not intended to be exhaustive or all-inclusive.

Baseline Mask	Pattern of the spectrum of frequency amplitudes when new or at a starting point
Peak Hold Spectrum	The spectrum of the highest amplitude in each bin/line/filter for however long the "averaging" takes, or number of averages. The amplitude depends on the selected scale, and it could be RMS or Peak or Peak-to-Peak or dB.
Modulation	Amplitude modulation is defined as the multiplication of one time-domain signal by another time-domain signal. Either or both signals may contain harmonics components. The signals may be electrical in nature, or they can be vibration signals. Modulation is inherently a non-linear process, and always gives rise to frequency components that did not exist in either of the two original signals
Amplitude Demodulation	The process of discerning a signal from its carrier signal, and is similar to AM radio, where the carrier is a high frequency signal generated by the radio station, and the modulating signal is the voice or music that constitutes the program. The radio receives the modulated carrier, amplifies it, and rectifies ("detects") it to recover the program.
Harmonic	A harmonic is defined as an integer (whole number) multiple of the fundamental frequency
Nyquist Frequency	Named after the Swedish-American engineer Harry Nyquist, is half the sampling frequency of a discrete signal processing system. It is sometimes known as the folding frequency of a sampling system.
Octave Spectrum	The frequency range of interest is divided into set of frequencies called bands. Each band covers a specific range of frequencies. IN this regard, a scale of octave bands and one-third octave bands has been developed. A frequency is said to be an octave in width when the upper band frequency is twice the lower band frequency. A one-third octave band is defined as a frequency band whose upper band-edge frequency (f_2) is the lower band frequency (f_1) times the cube root of two.
Cepstrum	Cepstrum Analysis is a tool for the detection of periodicity in a frequency spectrum. The Cepstrum is defined as the power spectrum of the logarithmic power spectrum.
Rahmonic	Rahmonics are cepstral components that are spaced at equal increments of time.
Order Tracking	Order tracking synchronizes the sampling of input signals to the instantaneous angular position of the machine shaft using a resampling technique. Rather than a constant number of samples per time, this results in a constant number of samples per revolution and transforms the analysis to the order domain rather than the frequency domain.

SUMMARY

A significant opportunity for improving power generation availability within New York State and throughout the country can be realized by improving the availability of wind turbine generators. While original equipment manufacturers (OEM's) sometimes offer a form of vibration-based fault diagnostics and health prognosis system—with several third-party aftermarket systems also available—two key problems remain:

- First, the signal processing techniques employed by such systems do not adequately address the complex nature of the vibration signals emanating from a gearbox with multiple gears and bearings spinning at a variety of speeds and loads, both varying over relatively short timescales. For example, many systems are programmed to hunt for spectral peaks at key gear mesh frequencies. However, because of modulating effects inherent to the vibratory nature of interacting gears, these spectral peaks are not always located in the baseband, but rather appear as sidebands of other related frequencies such as shaft speeds.
- Second, all available systems utilize vibration transducers mounted on the gearbox and other components in the nacelle. As discussed in more detail later, access to the nacelle for equipment health monitoring is a problem. Specifically, expensive data acquisition and communications hardware may not even be allowed to be installed in the nacelle, depending on liability insurance regulations as well as warranty and other business arrangements between the owner, operator, and OEM.

Because of these two issues, there remains a critical need for a vibration-based machinery fault diagnostics and health prognosis system that can properly and reliably interpret wind turbine gearbox vibration signatures, but is less invasive and expensive to install than nacelle-based systems.

The technical basis for this project was a ground-based data measurement system that remotely measures vibration. Specifically, a single piezoelectric accelerometer is mounted on the tower wall near the foundation to measure vibration originating within the nacelle. Work performed in this project has established the feasibility that advanced analysis methods, which are not employed by currently available predictive health monitoring systems, are able to: account for transmission effects added to the signal as it travels from the source down the tower; accommodate turbine speed and load fluctuations during the measurement; and separate the signal into components related to the main rotor, gearbox, and generator. The system developed separates signals and analyzes them for faults that can be monitored over time to track the degradation of key components, and provide the operator with useful trend information - similar to what is currently promised by marketplace solutions, but with improved portability, reliability, and lower

cost. Mechanical Solutions, Inc. (MSI) performed this assessment using structureborne vibration measured at the wind turbine tower base, as depicted in Figure S-1.¹

The innovation verified in this project is two-fold: first, the measurement of vibration from a single remotely located transducer, and second, the signal processing techniques to divide the vibration signal into the separate signals generated by main rotor, gears, and bearings in preparation for component-specific fault diagnosis and health prognosis.

The MSI system is less expensive and significantly less invasive than OEM-installed and aftermarket nacelle-based monitoring systems, both those presently available and those that the literature indicates are under development. Figure S-1 shows the system's hardware: A single piezoelectric accelerometer with magnetic base attaches to the tower wall near the foundation. A small signal conditioner powers the sensor, receives its signal and provides data to a standard laptop computer containing MSI-developed software to extract and process the data.

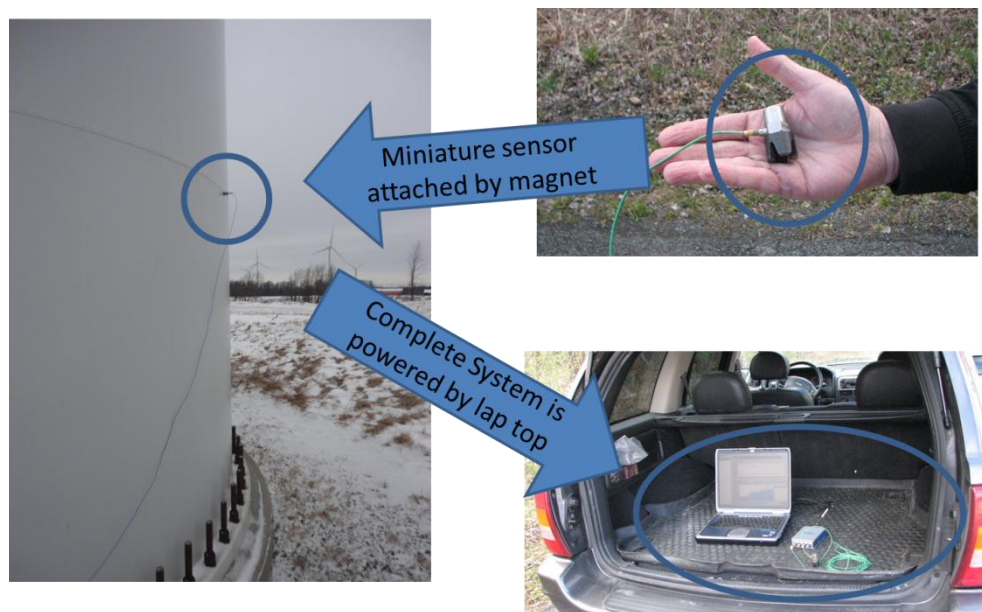


Figure S-1: Wind turbine tower instrumented with a piezoelectric accelerometer to measure vibration originating within the nacelle after propagating down the tower.

All hardware is available off the shelf. The value-added portion of the system resides in its computer software.

¹ In the project we also evaluated a ground-based microphone to assess airborne sounds for similar diagnostic information content. If feasible, a microphone-based approach, although less sensitive, would further simplify our system. To date we have not observed meaningful diagnostic data in the airborne data, owing perhaps to the fact that none of the turbines instrumented for test purposes exhibited significant mechanical issues and associated vibration with sufficient coupling between the nacelle and surrounding air for detection.

Compared to most turbine-generators that produce electric power, wind turbines present a special challenge for condition monitoring. First, their operation is highly variable in speed and load, because of a continuously changing wind velocity field. Second, turbines are spread miles apart with their drive trains positioned several hundred feet in the air. Finally, key machinery information such as bearing geometry and gear tooth count is often not known for wind turbine generator drive line components. Sophisticated machinery diagnostics without this information is a special challenge.

Exacerbating the uncertainty about machinery specifications is the fact that the turbine fleet at a given site, even if homogeneous in make and model, may feature combinations of gearbox components and gearbox varieties. Thus, every turbine-generator is unique, and so it is impractical for a signal processing expert to interactively harvest frequency-of-interest information from data collected on the drivetrain of every turbine at a particular farm.

With all the constraints unique to wind turbine condition monitoring, MSI developed a signal analysis methodology that accommodates speed and load changes, can be employed on vibration data measured at the tower base, and does not require intimate knowledge of machinery details. When combined with a baseline of vibration data, periodically collected subsequent data samples provide the user with an easy-to-understand overview of turbine health, and the samples can be trended to assess changes in condition over time.

A prototype *MSI Wind Turbine Pro*^{TM2} system has been assembled and used to collect data from operating turbines. Although the data sample to date is rather limited, first results are encouraging and user feedback has been positive.

The work accomplished in this project has established the feasibility of using base-of-tower structural vibration to make first-order determinations regarding the running condition of a wind turbine's drivetrain components. On-going and planned work includes providing prototypes to interested users for test and evaluation, and system updates as appropriate. Migrating to tablet style computers is a future option as the capability of those devices progresses. Continued development offers MSI a unique opportunity to make significant and timely contribution to the wind turbine industry to effectively increase the availability of wind turbines, reduce greenhouse gases, and use/advance the technology and industrial base in New York State.

² Trade Mark applied for.

Section 1
INTRODUCTION

This report documents the work performed under NYSERDA Agreement 18800 “Non-Intrusive Predictive Health Monitoring for Wind Turbine Generators.” As a feasibility study under Program Opportunity Notice (PON) number 1670 “Environmentally Preferred Power System Technologies”, the primary objective of this project was to investigate the practicality of using structural vibration at the base of an operating wind turbine’s tower to determine the running condition of machinery in the turbine’s nacelle.

This study was performed by Mechanical Solutions, Inc. (MSI). Founded in 1996, MSI is a recognized leader in the development and application of practical methods to determine the condition of rotating machinery using vibration methods. For the purposes of this study, MSI utilized several existing items and extracted others from recent and on-going work, including the underlying essence of several vibration processing methods, the foundation of an initial user interface, and an in-house gear and bearing test rig. Concepts and scientific methodologies for this parallel work came from related developmental work being performed by MSI for the US Air Force under contract number FA9101-09-C-0024 “Rotating Machinery Health Monitoring”.³

Section 2 of this report relates use of and findings from the in-house test rig. Section 3 presents data acquired from operating wind turbines. Section 4 contains a summary of computer analysis of a wind turbine tower, to quantify the anticipated influence and transmission loss/distortion the tower may impart on vibration as it transits from top to bottom. Section 5 describes a prototype system to acquire and process base-of-tower structureborne vibration data, and Section 6 summarizes initial use of the system and related work in transferring the technology for use. Section 7 relates the conclusions and recommendations resulting from the work accomplished under this agreement.

³ Contract FA9101-09-C-0024 was a Phase II Small Business Innovative Research (SBIR) contract being administered by the USAF Arnold Engineering Development Center (AEDC). It was preceded by a Phase I contract that demonstrated the feasibility of several advanced methods to determine the functional health of specific AEDC equipment items. Under separate Phase I and II contracts MSI also produced a functional acoustic and vibration-based predictive maintenance system applied to AEDC brine pump chillers.

Section 2

IN-HOUSE TESTS

This section presents an overview of the test set-up used to assess the vibration-based diagnostic algorithms developed in this project. The aim of this work was to observe faulty bearings and gears.

TEST RIG

Figure 2-1 shows the rig as it existed at the outset of this project. The rig was initially built to test algorithms MSI was developing for the U.S Air Force⁴. As configured, a 20 hp wound rotor motor drove through a speed increasing gearbox to drive a multistage blower.

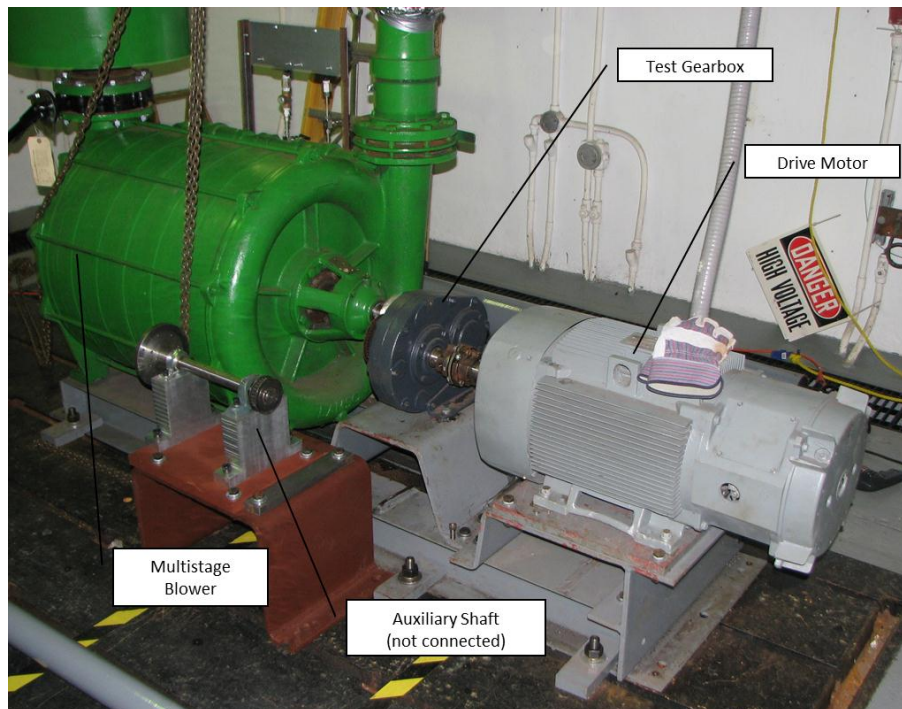


Figure 2-1. Gearbox Test Rig at MSI. Motor (1,800 rpm) drives through 2:1 speed increasing gearbox to a 3,600 rpm air blower. The blower merely provides a load for the gearbox and motor. The test rig was constructed as part of MSI's cost share for this project.

⁴ Contract FA9101-09-C-0024; see related discussion in Section 1.

To simulate vibration transmission through a tube-like structure, the test rig was modified as shown in Figure 2-2. A 6 inch diameter tube was fitted between the test rig and the overhead structure of the test cell. The tube was instrumented on both ends with vibration sensors so their signals could be compared to assess transmission loss and signal distortion. Figure 2-3 shows an overall view of the test rig as finally configured.



Figure 2-2. Wind turbine tower simulation tube (a length of 6 inch diameter pipe), right, was installed on test rig. The tube (later welded top and bottom) was instrumented on both ends with vibration sensors so their signals could be assessed for predicted vs. measured transmission loss and distortion. The thinner vertical tube at left was later removed from the test set-up.



Figure 2-3. In-House test rig as finally configured. Not shown is vibration sensor at top of Tower Simulation Tube.

TEST DATA

The test stand was set up for 24/7 unattended operation. For vibration monitoring, the rig was originally outfitted with a 4-channel MSI-owned data acquisition system. This was later replaced, first with the data collection hardware for the prototype Wind Turbine Pro™ system, then pre-release versions of the system's software. This provided a convenient means to check out the prototype system in-house. Data collected provided important information to both the NYSERDA and the parallel Air Force projects. Figure 2-4 shows typical vibration data recorded during the test program.

GEARBOX MODIFICATIONS

Although the rig's gearbox was intentionally run with decreasing amounts of lube oil, no naturally occurring gear or bearing faults were observed through more than 3,000 hours of operation. This was attributed to the fact that the gearbox was loaded to only 5% of its rated load. To confirm the system's ability to detect faulty gears and bearings, faults were installed on both, with good effect, as noted in Figures 2-5 and 2-6. Section 5 discusses the data obtained during these seeded fault tests.

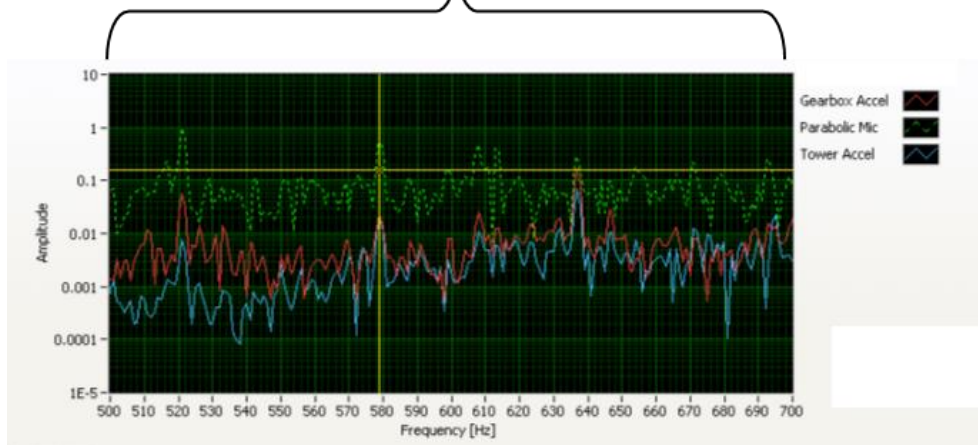
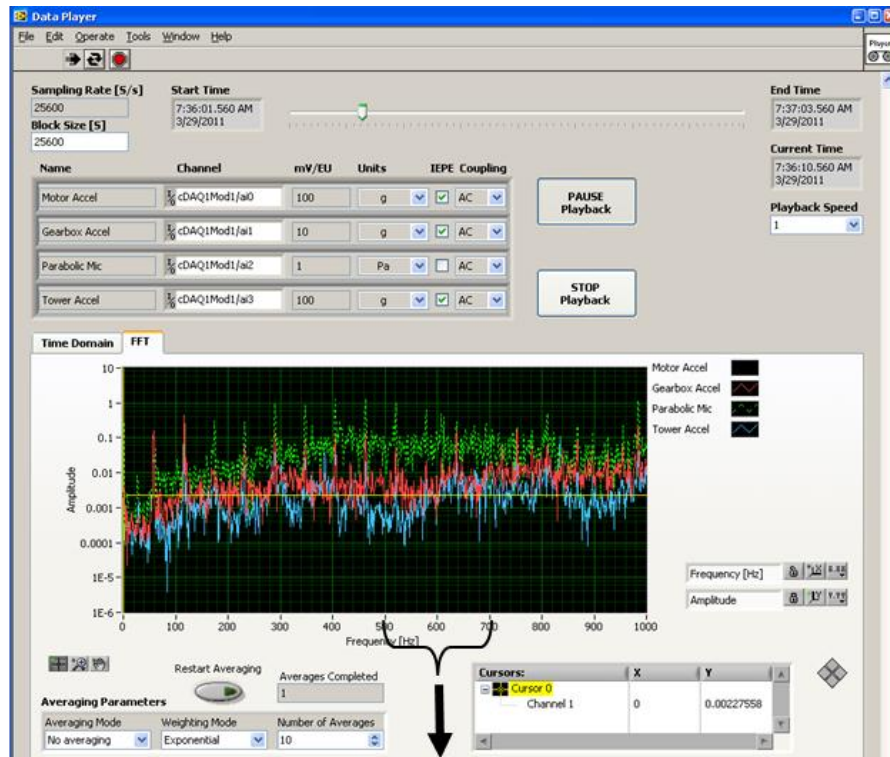


Figure 2-4. Test rig typical vibration data. Upper portion shows the user interface for the initially-implemented data collection system. The lower portion shows an enlargement of the vibration spectrum with several discrete frequency peaks including the gearbox's 577 Hz gear mesh frequency, where the cursor shows the amplitude (approx. 0.2 g) for the gearbox sensor. At this frequency, the sensor at the top of the Tower Simulation Tube (blue curve) was approx. 0.02 g. The parabolic microphone (dashed curve) also shows this and other machinery-related frequencies.

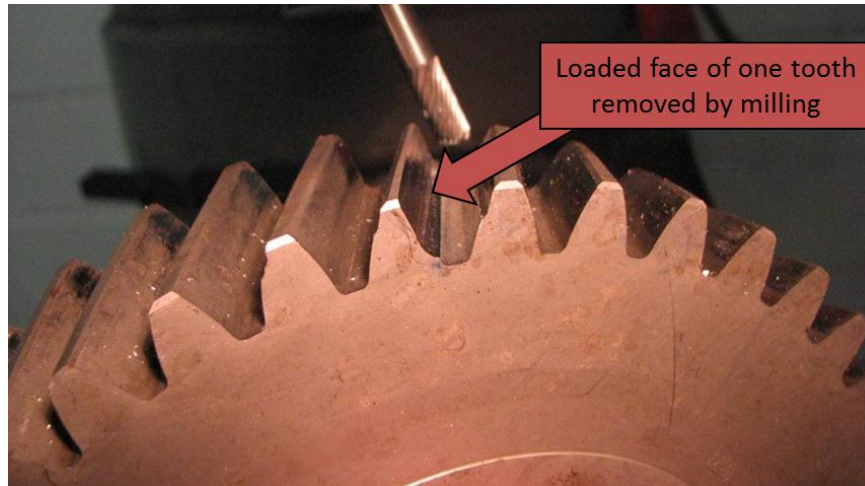


Figure 2-5. Tooth fault installed in one tooth. The loaded face was cut back so it would not intersect with mating tooth. The prototype system detected the fault as a change in balance. No change in gear mesh frequency was observed, probably since the gearbox was lightly loaded (approx. 5% of rated load), and only a single tooth (not a distributed fault) was modified.



Figure 2-6. First bearing fault installed in gearbox bearing. Fault was detected by the prototype system. The fault was later enlarged (doubled the width around the bearing) to represent end-stage failure. The bearing failed thereafter and caused collateral damage that ended the in-house tests.

Section 3
WIND TURBINE VIBRATION DATA

This section summarizes the measurement and assessment of data collected from operating wind turbines during the course of the project. The initial data, collected in May 2011, provided important insight regarding wind turbine machinery arrangement and site layouts. Based on this information, a refined set of data collection hardware and an updated test approach was implemented in February 2012. During each visit, acoustic (using a microphone mounted in a parabolic reflector) and up- and down-tower vibration measurements were made.

MAY 2011

A visit to the Noble Environmental Power North Country site near Plattsburgh, NY took place May 16–18, 2011. Two wind turbines were instrumented with MSI-owned equipment. Both up-tower and down-tower simultaneous measurements were made while the turbines operated normally, each for a 1-2 hour period. Although wind conditions were light and variable, valuable data was acquired. Figure 3-1 shows vibration spectra from the gearbox case (upper curve) and the tower base (lower curve) for the same instant in time. It was encouraging to see several key frequencies at both locations. It is important to recognize that the source labels on the figure are educated guesses only, as site personnel did not know gear tooth counts and other machinery-related specifics.

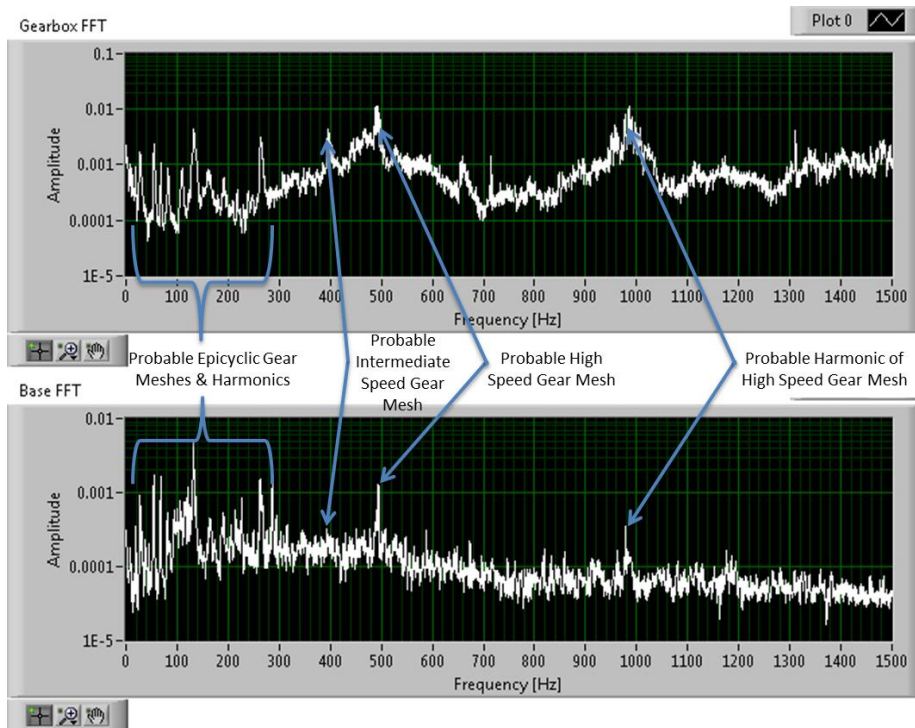


Figure 3-1. Comparison of up-tower vibration on wind turbine gearbox (upper curve) to simultaneous measurement of vibration at the base of the wind turbine tower (lower curve). Probable vibration sources are noted.

The acoustic data was less encouraging. Figure 3-2 shows data from a parabolic microphone positioned approximately 100 ft. from the turbine base and aimed up at the nacelle. The data was dominated by generator-related frequencies, with no gear or other drive train frequencies evident. Less sensitive than structurally attached sensors, the instrumented turbines did not exhibit significant mechanical issues and resulting vibration that could have resulted in the necessary coupling between the nacelle structure and surrounding air to allow detection.

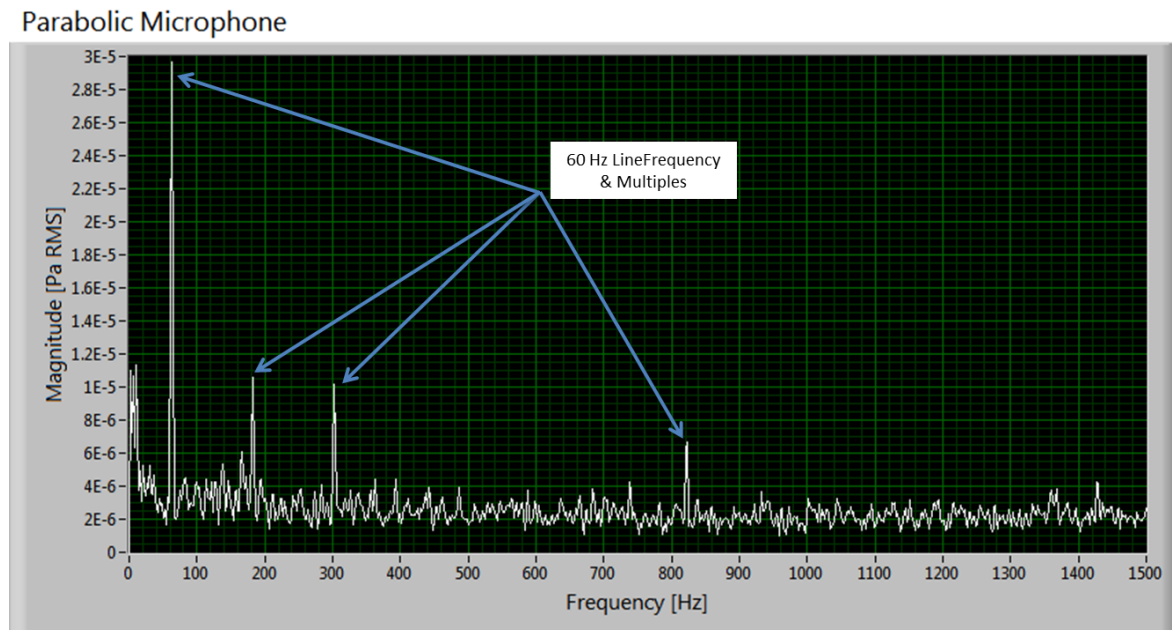


Figure 3-2. Vibration spectrum of airborne sound during wind turbine operation shows mostly electrical power-related frequencies.

FEBRUARY 2012

A second visit to the Noble Plattsburgh site took place January 31 – February 1, 2012. Seven wind turbines were instrumented – six with base-only sensors and one with both up- and down-tower sensors. Since they are geographically distanced from each other, multiple turbines were not measured simultaneously.

Base-Only Measurements

Wind conditions were light when the six base-only turbines were monitored. For these turbines a single vibration sensor was attached and data was recorded for approximately five minutes. Figure 3-3 shows the power levels for these turbines while being monitored along with the overall vibration level observed. Figure 3-4 shows a typical time waveform for these turbines. The occasional spikes were observed more frequently in some turbines than others and were determined to be related to nacelle yawing and blade pitching, the result of changing wind conditions. It became apparent that a meaningful diagnostic system needs to be developed to accommodate these types of events.

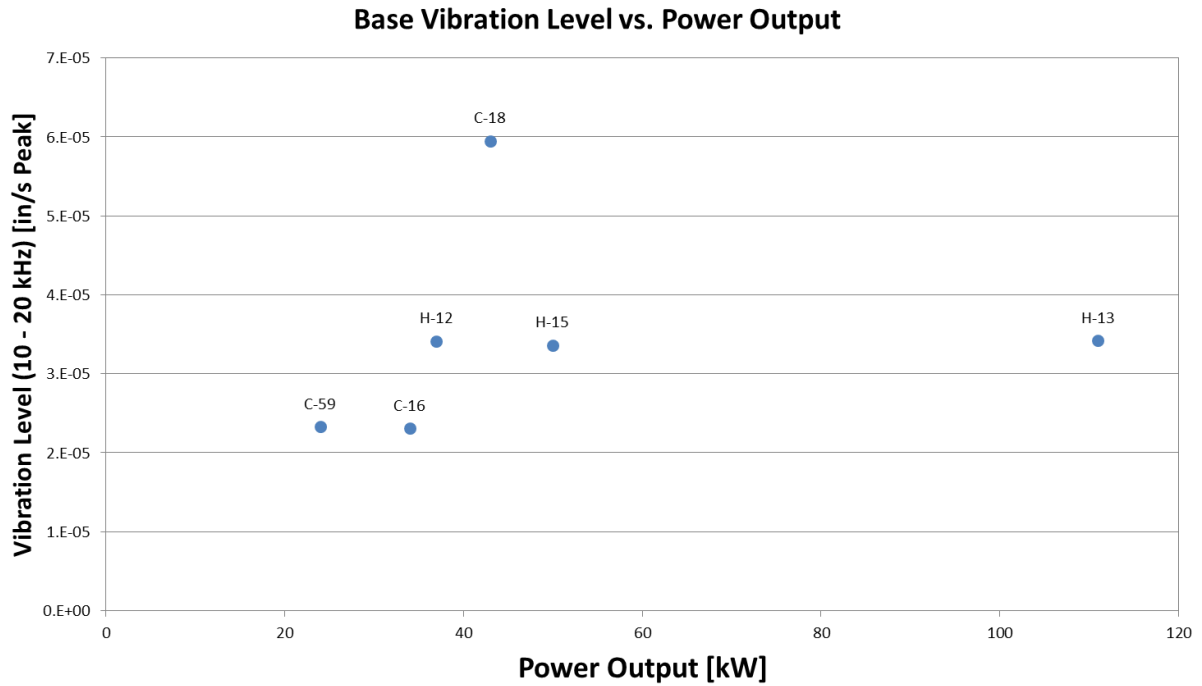


Figure 3-3. Comparison of overall down-tower vibration and power for six turbines.

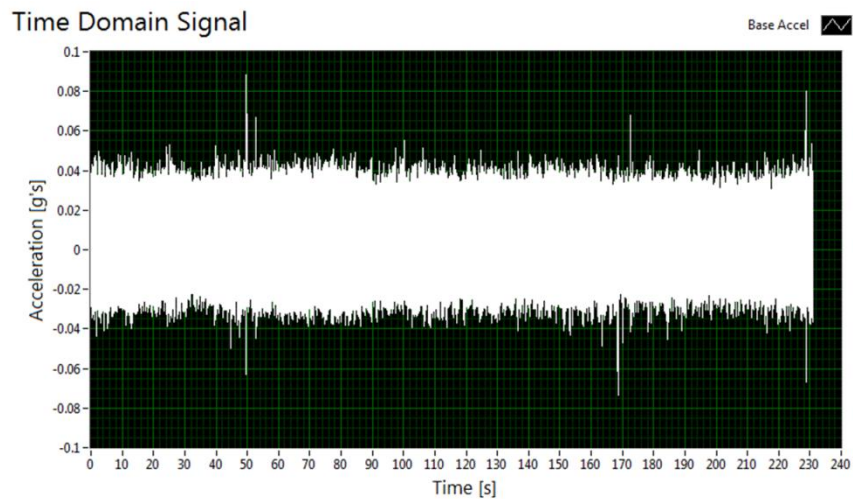


Figure 3-4. Turbine C-16 - Typical overall vibration amplitude vs. time waveform. Outliers are associated with nacelle yawing and blade pitching.

Up- and Down-Tower Measurements

Two sets of instrumentation, one in the nacelle and one at the base were installed on turbine E-49 and left in place overnight, acquiring data continuously. Figure 3-5 shows how the wind speed and turbine load varied during this time. As the figure shows, wind speed increased overnight and the turbine ran at nearly full power (1.5 MW) at times. Figure 3-6 shows the correlation between overall vibration at the base and

turbine power. This correlation confirmed the potential to extract meaningful data from sensors at the base. Figure 3-7 shows this comparison for two accelerometers on the tower base, located 90 degrees apart.

Figure 3-8 compares the vibration spectra for a sensor attached to the gearbox to a sensor at the base of the turbine tower. The spectral similarity in several regions (note logarithmic vertical axis) provided additional verification that diagnostic information can be gleaned from the sensors at the tower base.

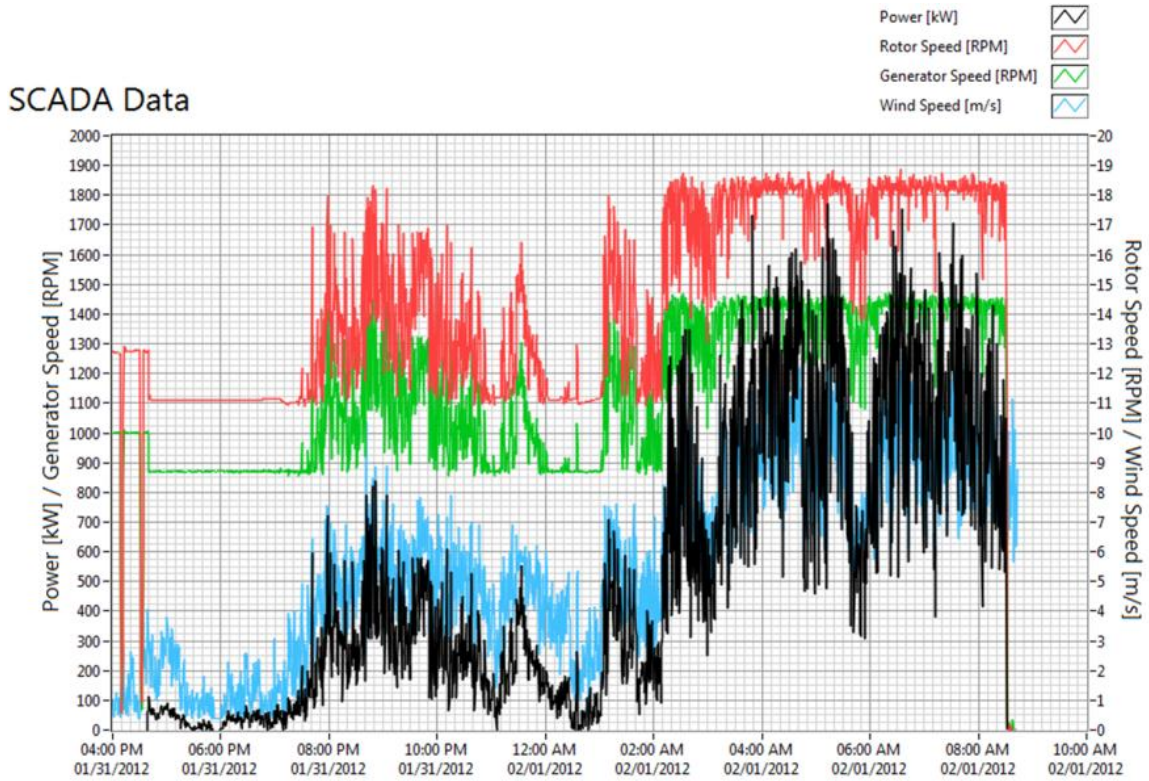


Figure 3-5. Turbine E-49 - Comparison of power, wind speed, generator speed and turbine speed for 16+ hours.

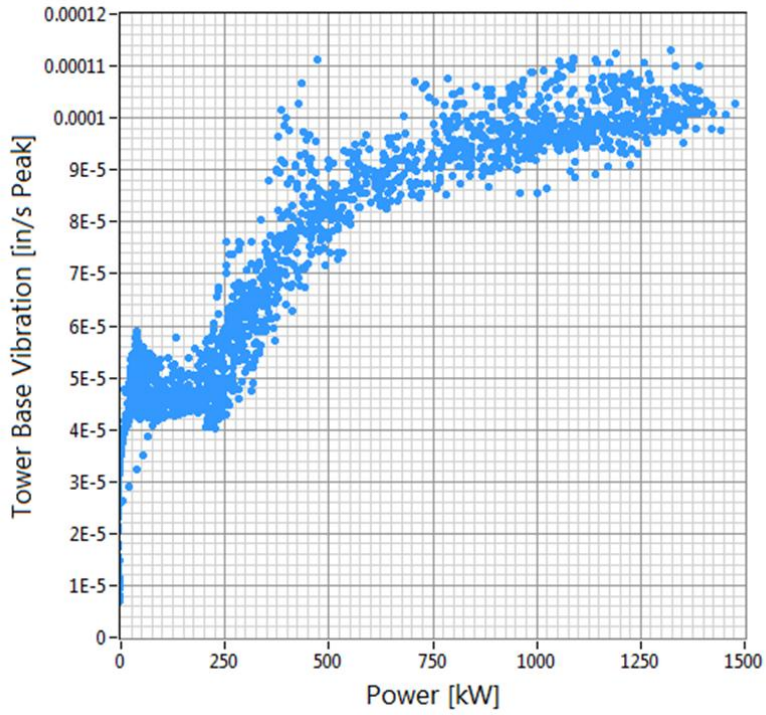


Figure 3-6. Turbine E-49 - Correlation of overall vibration at tower base vs. turbine power.

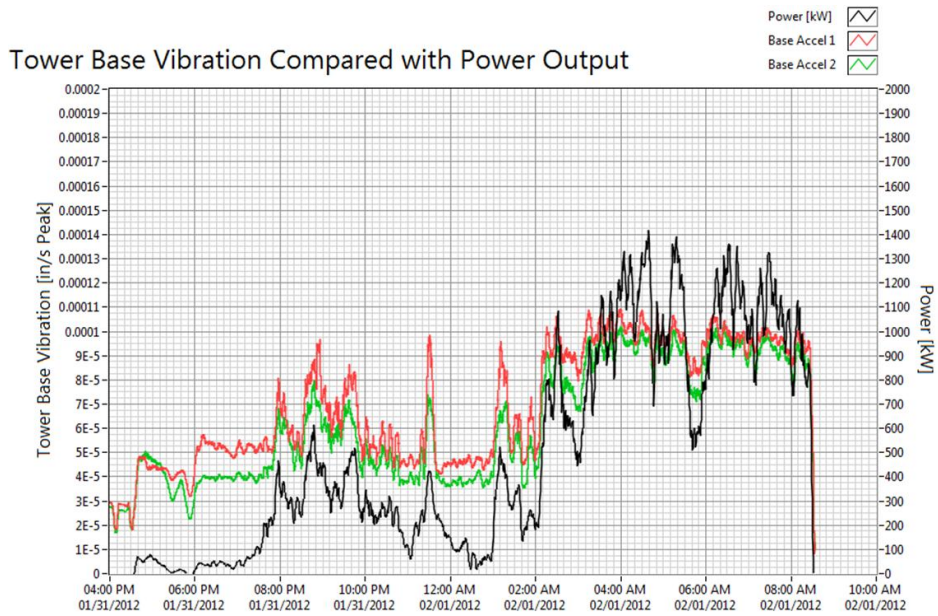


Figure 3-7. Turbine E-49 - Comparison of tower base vibration vs. turbine power for two tower base sensors placed 90 degrees apart.

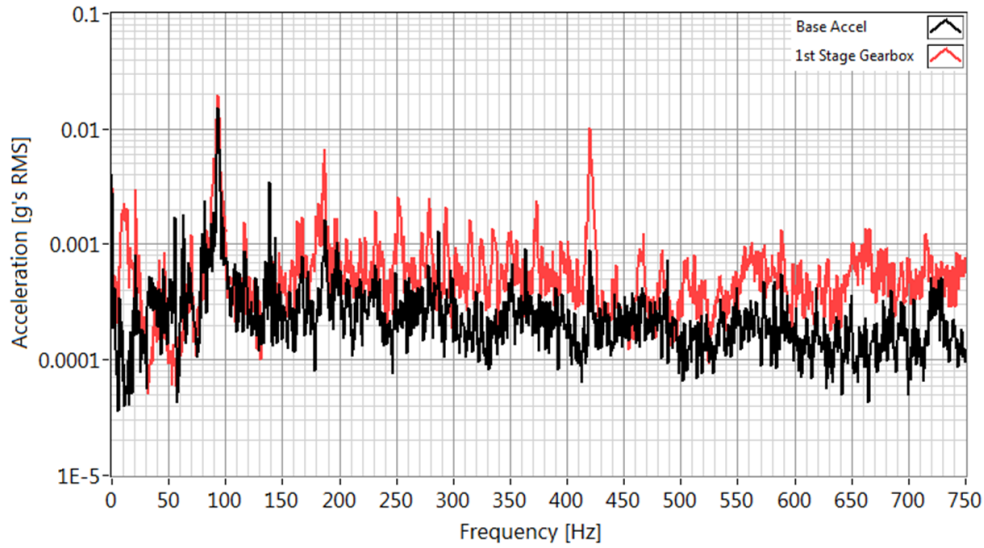


Figure 3-8. Turbine E-49 - Comparison of up- and down-tower vibration.

Acoustic Measurements

Figure 3-9 compares a typical acoustic spectrum as measured adjacent to turbine E-49 (see Figure 3-10 for set-up) to an accelerometer mounted to the base. As a measurement method with lower sensitivity, it was concluded that there was no significant diagnostic data in the acoustic signal.

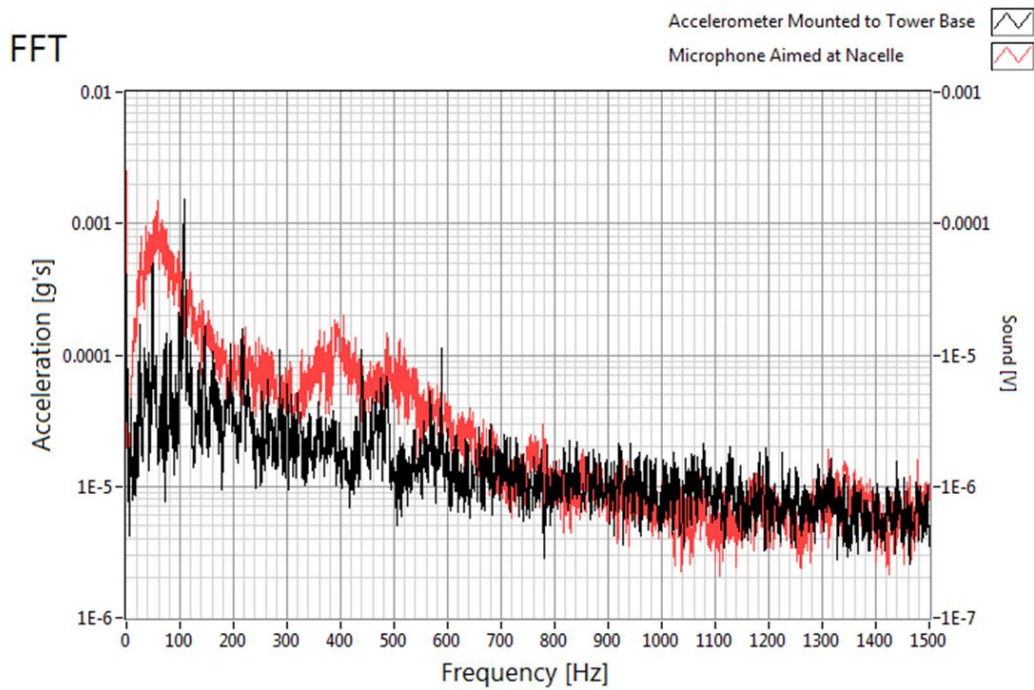


Figure 3-9. Turbine E-49 - Comparison of acoustic and down-tower vibration data.



Figure 3-10. Turbine E-49 – Acoustic measurement set-up using a microphone and parabolic reflector about 100 feet from the tower.

Data Assessment

Combined with the results of computer modeling of the structure of a typical wind turbine in this size range (see Section 4) and an assessment of the vibration data collected from these turbines, MSI concluded that a novel data analysis method was warranted. As described in Section 5, the method implemented in the prototype MSI Wind Turbine Pro™ system involves using the constant percentage bandwidth (CPB) spectrum, also known as a fractional octave spectrum, instead of typical analysis methods based on discrete frequency identification and tracking, as historically implemented in vibration-based machinery monitoring systems. We also decided to forego, at least initially, inclusion of vibration-derived statistics-based values (Root Mean Square (RMS), average, Kurtosis, etc.) originally considered for this system. These decisions were based on a combination of MSI experience in this technology area and discussions with consultant Robert Randall, Ph.D. Dr. Randall is Emeritus Professor at the School of Mechanical and Manufacturing Engineering, University of New South Wales, in Sydney, Australia, and an internationally recognized authority in advanced algorithms for vibration assessment. Under MSI purchase order, Dr. Randall and his colleague Nader Sawalhi, Ph.D.⁵, reviewed the wind turbine vibration data MSI provided. Appendices A and B contain the reports submitted by Drs. Randall and Sawalhi. In addition to these summaries, Dr. Randall and MSI staff met face-to-face for extended discussions and data reviews in May 2011 (at the annual meeting of the Machinery Failure Prevention Technology meeting in Virginia Beach, VA) and in February 2012 (at MSI headquarters).

⁵ Dr. Sawalhi is a former student of Dr. Randall and is currently Assistant Professor, Mechanical Engineering Department, Prince Mohammad Bin Fahd University (PMU), AlKhobar, Saudi Arabia.

Section 4 TOWER ANALYSIS

The focus of this work was to use finite element analysis (FEA) to study wind turbine vibratory characteristics and provide insight as to how structureborne vibration measurements taken at the base of the tower could be used for diagnostic/prognostic analysis efforts.

INITIAL MODEL

Work started with a simple model using MSI-measured dimensions of a GE 1.5 MW wind turbine at Noble's North Country wind park, see Figure 4-1. The simplified model, which consisted only of the tapered tubular tower simply supported at one end, was used in a series of modal super-positioned harmonic analyses subject to forcing functions representative of different gear faults. An examination of the frequency response function (FRF) of lateral acceleration at the base of the tower indicated that even for high levels of damping it would be theoretically possible for gear mesh forcing functions to be measured by an accelerometer at the base of the tower given sufficient amplitude.

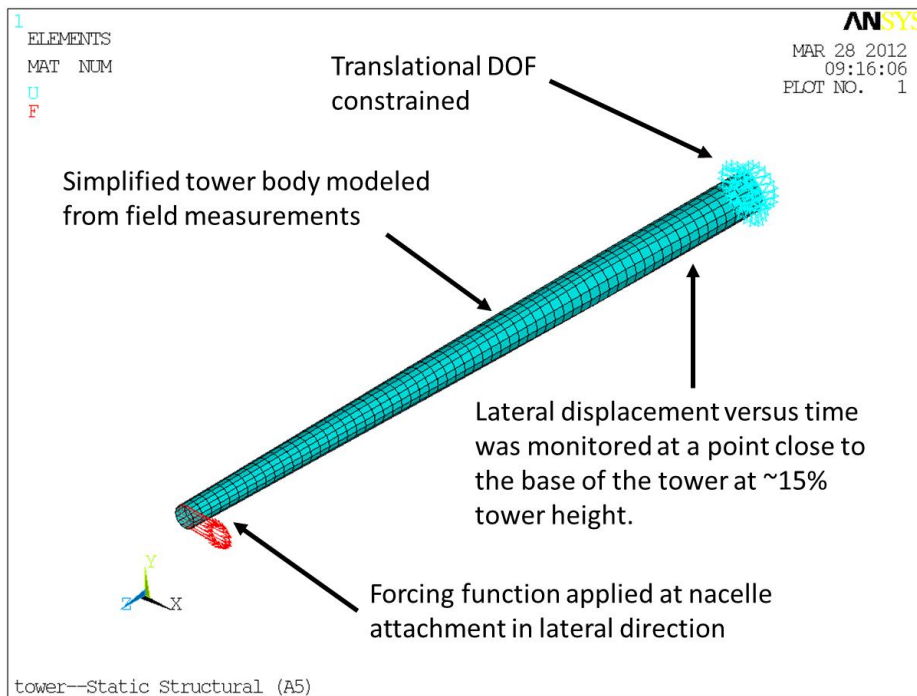


Figure 4-1. Initial (simplified) finite element model of a wind turbine tower.

SUBSEQUENT MODEL

The results of the simplified model encouraged construction of a more detailed model with higher fidelity for further study. A more thorough research effort was conducted to gather as much publically available information as possible on the same wind turbine model and its internal components. Length scales, weights, vibration isolation supports, and component mounting were estimated from a variety of available information and combined with physical measurements taken by MSI in the field for the same model. Finally, a detailed wind turbine FEA model was produced complete with concrete foundation and rotating components, see Figure 4-2. This model was then used in a similar manner as the simplified model by subjecting it to forces typically observed in faulted gears.

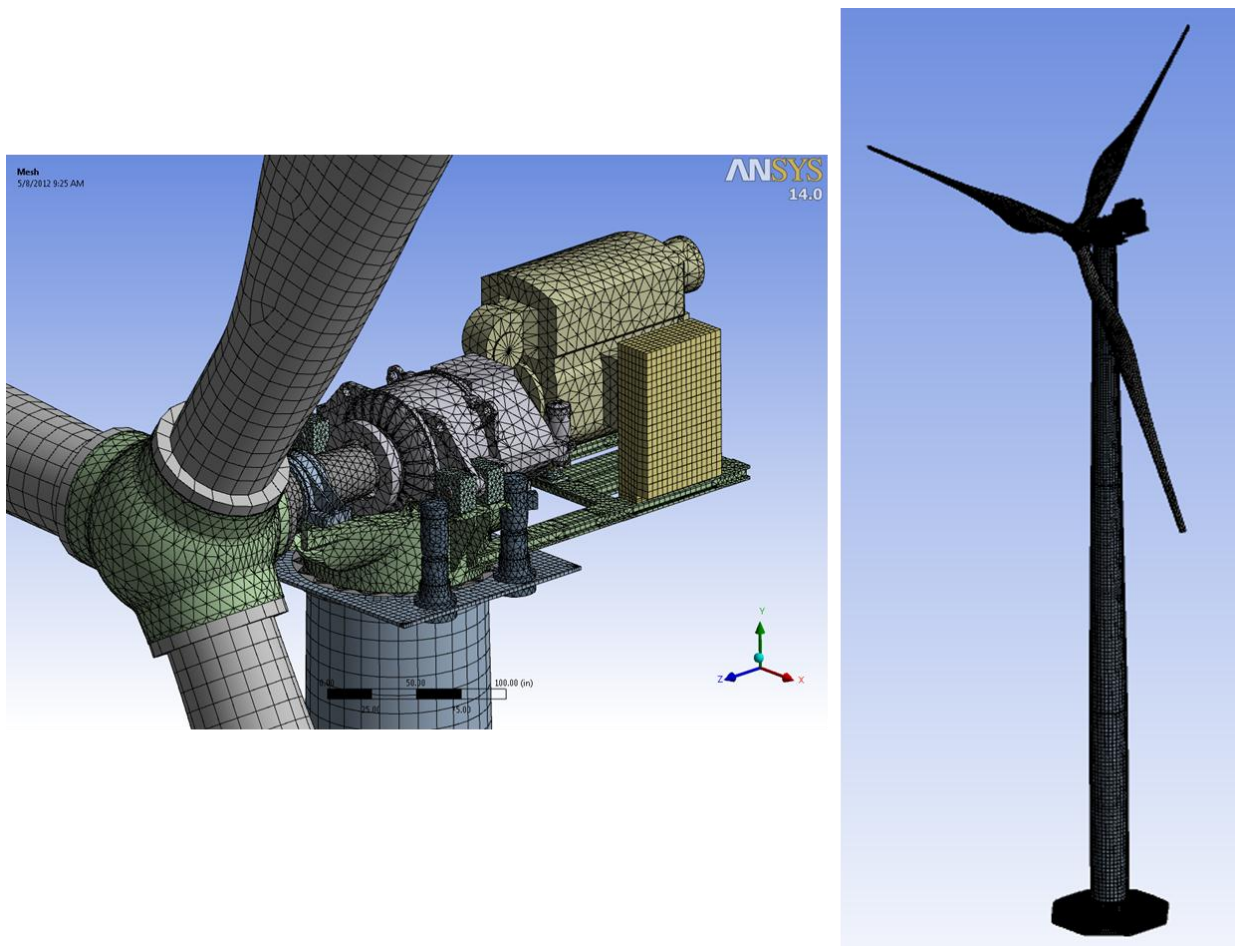


Figure 4-2. Subsequent (detailed) finite element model of a wind turbine, consisting of approximately 1.5 million degrees of freedom. The generator (with air cooler on top) is shown at the right end, with the 3 stage gearbox in the center, and turbine at the left. All components mount to a common sub-base. Multiple yaw drives (2 shown) reposition the nacelle as wind direction changes. A control cabinet sits alongside the generator.

The first forcing function was intended to simulate a 22 tooth gear rotating at 1,440 rpm (24 Hz) with a singular damaged gear tooth. This *concentrated fault* results in a forcing function comprised of a single sine wave representing the healthy gear mesh and a low duty cycle impact in place of the damaged tooth. Fourier decomposition of this waveform results in spikes of harmonic content in multiples of 24 Hz whose amplitudes increase and fall every few thousand Hz (depending on the impulse width) and the addition of a discrete peak at the gear mesh frequency ($22 \times 24 = 528$ Hz). When this forcing function was applied to the gearbox as a bulk mass, the resulting acceleration vs. frequency monitored at the base of the tower (representative of what an accelerometer would measure) shows a very active Frequency Response Function (FRF) due to the large number of complex wind turbine modes in that frequency range. By increasing the magnitude of the force for the faulted tooth and keeping the remainder of the healthy gear mesh signal the same, the broad band noise floor for the forcing function increased (the discrete gear mesh peak remained unchanged), and the same happened for the FRF.⁶

The next forcing function investigated was one intended to represent the same gear with a *distributed fault* which in the time domain results in an amplitude-modulated sine wave. Fourier decomposition of this function results in a discrete peak at gear mesh (528 Hz) with two discrete side bands separated from the gear mesh peak by the 24 Hz shaft running speed. With this forcing function again applied to the gearbox as a bulk mass, the FEA showed this content in the FRF at the simulated probe location with similar side peaks.

A take-away here is that there is value in knowing the true transfer function of a structure, which can be used to help understand what actual forces may be acting at another location, even if it is quite far from the measurement point such as in the case of the nacelle-to-tower base.

Transfer functions can be determined either analytically with a high fidelity model such as that presented here, or via impact test measurements on the actual structure. Once the transfer function of interest is acquired, one can use the quotient of the transfer function and a measured accelerometer FRF to back-calculate the level of force acting in the nacelle (such as the force exerted from a gear or bearing once identified) which can then be used for subsequent diagnostic/prognostic calculations.

Along with assessment of measured vibration data from operating wind turbines, the findings related here formed the basis for the data analysis approach used in the prototype Wind Turbine Pro™. That methodology is related in Section 5.

⁶ In fact, a subtraction of the change in the FRF and the change in the forcing function would have the same pattern. This is due to the fact that the measured response is simply the multiplication of the forcing function with the transfer function between the two points (measured point and forced point).

Section 5

PROTOTYPE DIAGNOSTIC SYSTEM

This section describes the prototype MSI Wind Turbine Pro™, the initial vibration-based, noninvasive, portable monitoring system MSI has developed to assess wind turbine operating condition. Preceding is a discussion of the particular attributes that resulted in the data processing methods employed.

SIGNAL PROCESSING

From a signal processing perspective, wind turbines can have several operational characteristics that present the vibration analyst with special challenges. An additional consideration is the desire to have a noninvasive, portable diagnostic system that is easy-to-use while still providing useful and reliable information regarding the running condition of up-tower machinery.

Considerations Unique to Wind Turbines

Wind turbines have distinctive characteristics for condition monitoring. First, their operation is highly variable in speed and load because of changing wind speed and direction. Second, neighboring turbines can be miles away, and their drive trains are located hundreds of feet in the air. Finally, wind turbine operators may not know key wind turbine machinery information such as bearing geometry and gear tooth counts. In combination, these aspects make sophisticated machinery diagnostics a true challenge.

Speed Variability. In conventional rotating machinery vibration analysis, condition monitoring typically boils down to tracking the vibration magnitudes at several key running speed frequencies. Example frequencies include the shaft rotational speed and gear mesh frequency. With the majority of rotating machines operating at constant or near-constant speed, it is not difficult to track these vibration magnitudes and look for unexpected changes to diagnose problems. On the other hand, a wind turbine frequently changes speed (see Figure 3-5 for example). Since it is common for wind turbines to include step-up gearboxes with speed ratios of 80:1 or more, a change in main rotor speed of just a few rpm translates to a range of several dozen Hz for other key running speed vibration frequencies. Even when running at full speed, turbine rpm can still change enough to shift gear mesh frequencies by several Hz.

Analysis techniques exist that enable automated tracking of vibration magnitudes synchronous to a variable running speed, but these require a tachometer or encoder to precisely measure shaft speed. Given the desire for non-intrusive measurements at the tower base, these signals are not available. Although techniques for normalizing

vibration data with respect to speed without a tachometer or encoder exist, they are not readily automated⁷. Therefore, MSI sought a signal processing algorithm that is both independent of, and resistant to, speed variations.

Load Variability. For the same reason that wind turbines operate under changing speeds, they also operate under changing loads, both torsional and lateral. This is again a departure from most conventional rotating machinery applications where the load is either fixed, or at least changes in known discrete amounts.

Vibration magnitudes synchronous to running speed are typically dependent on the machine's load. The exact relationship can be proportional, inversely proportional, or nonlinear. For example, vibration at gear mesh frequency may decrease under high load and increase under light load. If the relationship between vibration magnitude and load is known for a particular running speed harmonic - either from testing or analysis - then the expected vibration magnitude can be computed from the measured load. Departures from the expected magnitude can be used to diagnose problems. For wind turbines, load could be invasively measured using strain gages on the shaft, or more crudely and qualitatively, using an external anemometer. In either case, it is again impractical to assume that load information is available to a non-intrusive measurement system operating at the tower base. Therefore, MSI sought a signal processing algorithm that does not require knowledge of wind turbine load.

Measurement Accessibility. Wind turbines can be situated miles apart from each other, and their drive trains are elevated several hundred feet in the air. There are several approaches to collecting condition monitoring data given the geographic and elevation challenges. One the one hand, every turbine at a wind farm could be instrumented with permanently-installed transducers cabled to a data acquisition system residing either in the nacelle or at the tower base. Modern communications equipment can be configured for remote access to the data acquisition system from nearly anywhere in the world. However, duplicating instrumentation and data acquisition hardware for each turbine is expensive, installation is labor-intensive, and sensor system maintenance an added workload. In this regard, the cost and complexity of outfitting one wind turbine (1 or 2 MW capacity) with permanent condition monitoring instrumentation is about the same as needed for a single steam turbine train (1,000 MW capacity). The installation would need to be duplicated for every wind turbine at a particular wind farm.

On the other hand, a wind farm could invest in a portable data acquisition system to carry from turbine to turbine to collect data snapshots for analysis. Even so, if each snapshot required one or two round trips up to the nacelle, which typically takes at least one hour per round trip and requires turbine shutdown, this approach would quickly become unattractive. Thus, collecting data at the base of the tower has enormous advantage, even if the result is merely first-order health indication of up-tower machinery.

⁷ One example is phase demodulation, which uses information contained within the vibration signal itself to account for speed variations. Unfortunately, this technique is only successful under certain conditions, and typically requires user interaction.

Machinery Uncertainty. As previously mentioned, most conventional rotating machinery condition monitoring involves tracking vibration magnitudes at key frequencies and looking for anomalous patterns in the trends. In today's wind turbine industry however, it is especially difficult to gather the information⁸ required to compute the key frequencies of interest to track, since it is often closely held by turbine providers. Although advanced vibration analysis techniques allow educated guesses at this information, they are not perfect and cannot be automated. Furthermore, the best results require a snapshot of vibration data collected directly on the drivetrain within the nacelle, which is impractical to repeat for every turbine at a particular farm.

Exacerbating the machinery uncertainty is the fact that the turbine fleet at a given farm, even if homogeneous in make and model, will likely consist of combinations of several gearbox and generator varieties. This is an inconvenient reality of the wind turbine supply chain. Thus, every turbine is unique, making it impractical to compile frequency-of-interest information on the drivetrain of every turbine at a large wind farm. Therefore, MSI sought a signal processing algorithm that is generically applicable to wind turbines, while being able to incorporate turbine-specific items if available.

Constant Percentage Bandwidth Spectrum

To accommodate the unique wind turbine aspects noted above in a condition monitoring system that would nonetheless provide meaningful information to the user, MSI collaborated with Dr. Randall, as noted in Section 3. The goal of this work was to develop a signal analysis methodology that is resistant to speed and load changes, that can be employed on vibration data measured at the tower base, and that does not require intimate machinery details. The approach resulting from our joint effort employs a constant percentage bandwidth (CPB) spectrum, also known as a fractional octave spectrum.

A CPB spectrum is similar to a traditional Fast Fourier Transform (FFT) spectrum in that it is a frequency domain representation of a time waveform. However, whereas an FFT spectrum sorts vibration magnitudes into frequency bins of equal width (i.e. data points are evenly spaced on the frequency axis), a CPB spectrum uses ever-wider frequency bins when sorting vibration magnitudes (i.e. data points are increasingly farther apart on the frequency axis as frequency increases). FFT spectra are typically plotted along a linear frequency axis, while CPB spectra are typically plotted along a logarithmic frequency axis, as seen in Figure 5-1.⁹

⁸ This information is typically comprised of bearing dimensions and gear tooth counts.

⁹ See Appendices A and B for summaries of Dr. Randall's work.

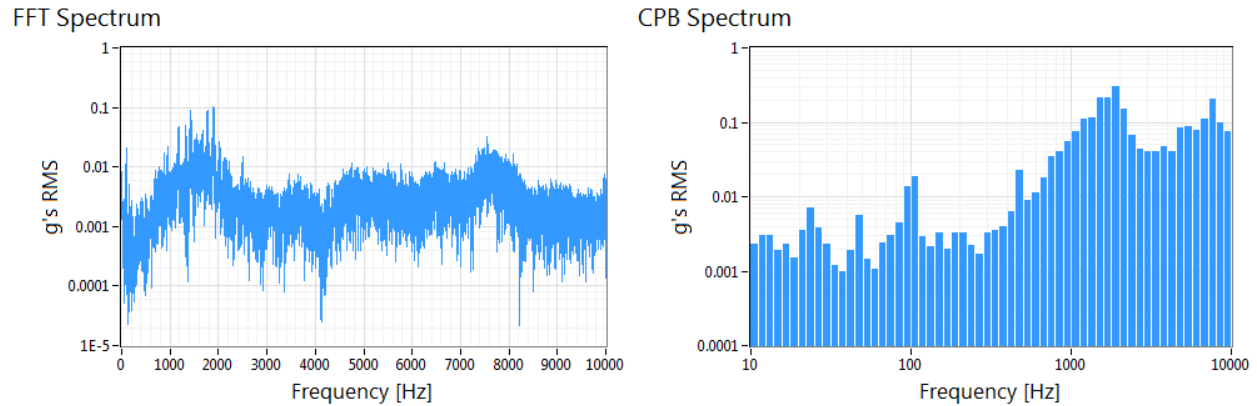


Figure 5-1. Comparison of a typical FFT spectrum and a CPB spectrum for the same data.

Note that the CPB spectrum has the same number of bins describing the signal content between 10 and 100 Hz as it has describing the signal content between 1,000 and 10,000 Hz. This makes the CPB spectrum resistant to speed changes. For example, any vibration between 95 and 105 Hz (a span of 10 Hz) is described as the aggregated height of the bar centered over 100 Hz. Similarly, any vibration between 950 and 1,050 Hz (a span of 100 Hz) is described as the aggregated height of the bar centered over 1,000 Hz. Vibration synchronous to a variable running speed lends itself well to be quantified in this fashion. The higher the harmonic number of a given vibration source, the more that signal component will change in frequency as speed changes; yet it will be measured by a correspondingly wider frequency bin. When described by an FFT spectrum, a drifting frequency component will shift bins (a few bins if low frequency, and many bins if high frequency). When described by a CPB spectrum, that same shifting frequency component will remain in the same bin, regardless of whether its frequency is low or high.

Baseline Mask

Using this scheme, a baseline mask CPB spectrum is created for each monitored wind turbine. The baseline should be recorded during commissioning, after a rebuild, or at when beginning a condition monitoring program. It is created by averaging together successive CPB spectra in a peak-hold fashion for a period of time long enough for the turbine to pass through its entire rated speed and load range. By using peak-hold averaging, the baseline mask represents the highest vibration magnitude at each frequency bin. Future CPB spectra, collected on a periodic basis (e.g. weekly, monthly, quarterly), are compared with the baseline mask. The margin to baseline can be tracked for each frequency bin and used to estimate the health of drivetrain components. As a first order assignment of probably cause, the frequency range is parsed into three sectors: Less than 100 Hz for main shaft balance and alignment problems; 100 to 1,000 Hz for gear-related issues; and greater than 1,000 Hz for bearing problems. Thus, even without knowing specific bearing dimensions or gear tooth counts, the frequency range of a particular bin that is nearing or exceeding its baseline mask can be used to identify a deteriorating component and prompt further investigation, which could range from checking component temperatures to looking for debris in the lube oil to a more thorough vibration assessment using sensors mounted directly to the machinery in question.

There is one final step involved in the creation of a baseline mask before it can be used in comparison with future CPB spectra. To bolster this method's resistance to speed fluctuations, the peak-hold spectrum is adjusted such that the magnitude of each bin is taken as the maximum of itself and its nearest left and right neighboring bin. Ideally, speed changes are small enough such that synchronous vibration signal components remain within a single CPB bin. Inevitably, though, there will be circumstances where a running speed harmonic straddles two adjacent CPB bins, perhaps even drifting back and forth between the two bins. "Shifting" the baseline one bin left and right, then taking the maximum, ensures that this special case does not give rise to false warning indications when compared with future CPB spectra. The MSI software automatically includes this shifting adjustment.

Experimental Validation

As described in Section 2, seeded fault testing was performed using an in-house test stand. The set-up consisted of a motor driving a compressor through a gearbox. A steel pipe was welded to the foundation and overhead and used to simulate the transmission path of vibration traveling down a wind turbine tower. The experimental measurement location was at the ceiling end of the steel pipe to simulate acquiring data at the base of a wind turbine tower (see Figures 2-1 through 2-3). Two faults were introduced: first, a bearing race within the gearbox was heavily scored, and second, a gear tooth was removed. Prior to inducing these faults, a baseline mask was generated. The CPB spectrum method successfully identified the bearing fault, where frequency bins in the bearing fault region ($> 1,000$ Hz) increased towards the baseline. Interestingly, the CPB spectrum method identified the gear fault more strongly as a rotor imbalance because the missing mass of the tooth unbalanced the rotor enough for the frequency bin containing the 1X synchronous vibration to exceed its baseline.

SOFTWARE

For the prototype system, a computer software program that facilitates push-button creation of CPB baseline mask spectra, and CPB measurement spectra was created using National Instruments LabVIEW®. The software also provides an environment to compare measurement spectra to a baseline mask and track margin to baseline over time. The data is organized and presented on a turbine-by-turbine basis with a graphical User Interface (GUI) that is optimized for portable use. The program is intended to work with the commercially available hardware described in the next section.

Configuring Turbines

The user can add, edit, and delete turbines from the software setup. When a turbine is added, information including main bearing geometry, gearbox tooth counts, generator bearing geometry, and user notes can be input if available. While the CPB spectrum analysis method, as described above, does not require such information, the system has been designed to provide additional diagnostic insight if machinery details are provided. For example, knowledge of bearing geometry facilitates advanced bearing diagnostics, as discussed below. The software is written in a modular fashion, so creating alternative turbine configuration screens in future releases will be straightforward. Direct drive turbines, for example, would require different setup information.

The list of turbines need only be input once and is stored in a data file and automatically loads each time the software is launched. Turbines can be duplicated in the setup, facilitating the data entry process for sites with a large number of similar machines. The setup can be locked so that users cannot edit or remove turbines inadvertently. Figure 5-2 shows the screen where the user adds a turbine to the setup.

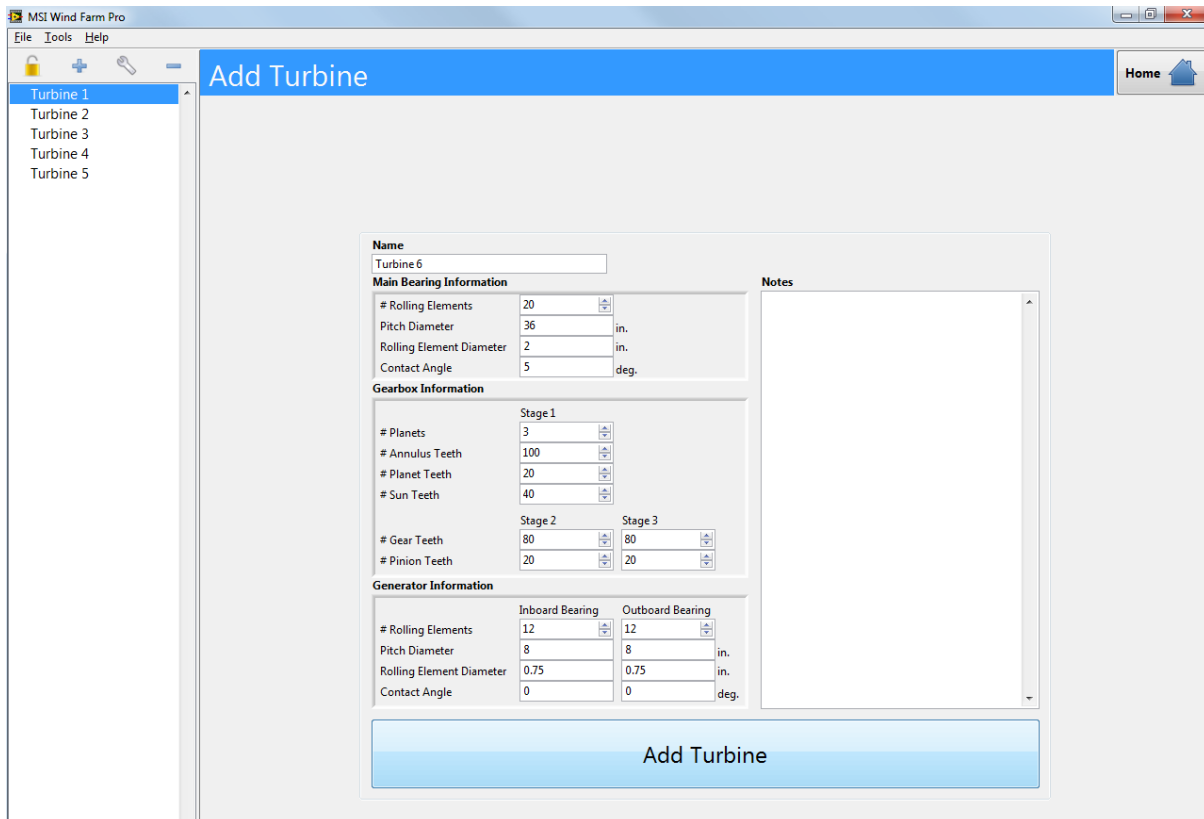


Figure 5-2: Adding a turbine to the setup.

Recording Baselines

Baselines are created individually for each turbine. When the user clicks to record a baseline, the software first prompts the user to place the accelerometer on the base of the wind turbine tower, as seen in Figure 5-3. After clicking to confirm the accelerometer is in place, the software initiates a baseline recording. The accelerometer time waveform scrolls across the screen as evidence of the signal. After the transducer and CPB filters settle, a CPB baseline characterization will also display on screen, as seen in Figure 5-4. The frequency range is demarcated as noted above, with fault regions for rotors, gears, and bearings. The recording process should last as long as required for the turbine to pass through its entire rated speed and load range. In this regard, it may be convenient to leave the system in place as it continuously gathers data, and return later. Once the user clicks to conclude the baseline, the software computes the mask by shifting each peak left and right and taking the maximum, as discussed earlier. The resulting mask is displayed to the user with the option to save or discard. Each turbine can have multiple saved

baselines, but only one can be active at any given time. The active baseline is the one used for comparing to newly recorded measurements for the turbine. The user can recall and notate past baselines to, for example, keep track of maintenance events that could alter turbine vibration performance.

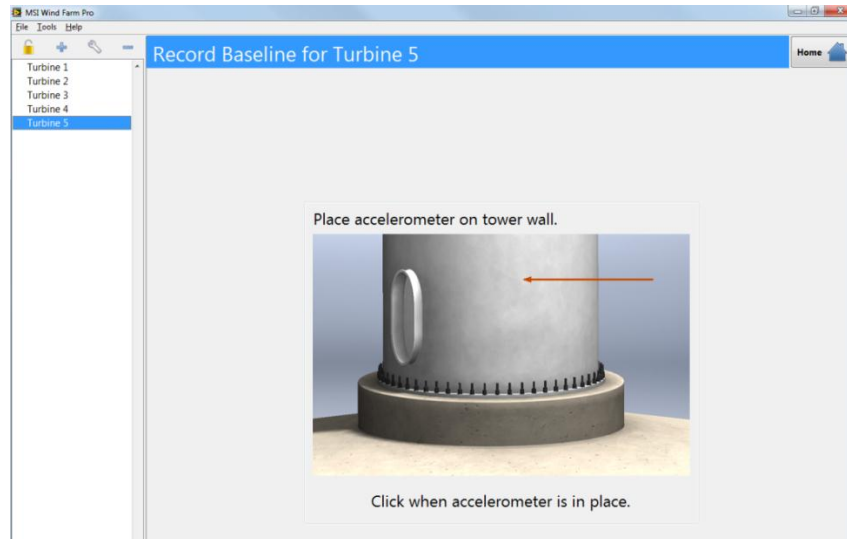


Figure 5-3. Preparing to record a baseline.

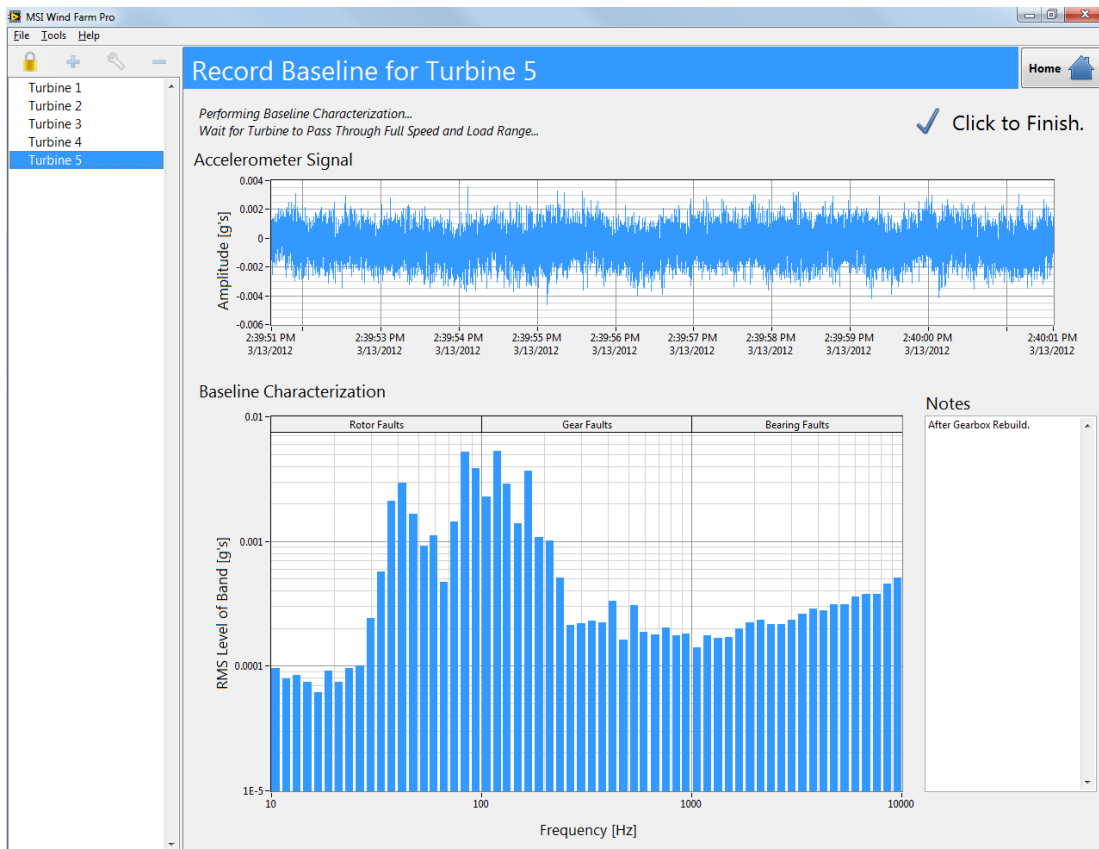


Figure 5-4. Recording a baseline.

Recording Measurements

Recording subsequent measurements is similar to recording baselines, but is a short “snapshot” of data. Turbine load may be any value during this time of course. The user is first prompted to place the accelerometer on the base of the tower. While the measurement is in progress, the software displays the current CPB spectrum overlaid on the baseline mask, see Figure 5-5. The baseline mask is shown as transparent blue bars, while the new measurement has solid blue bars. Should the measurement have bins that exceed the baseline, the excursions are graphed as solid red bars. The vertical axis can be set to a linear or a logarithmic scale. The software will automatically stop the measurement after sufficient data has been collected, say 30 seconds, and will bring the user to a screen where the new measurement can be compared to historical measurements.

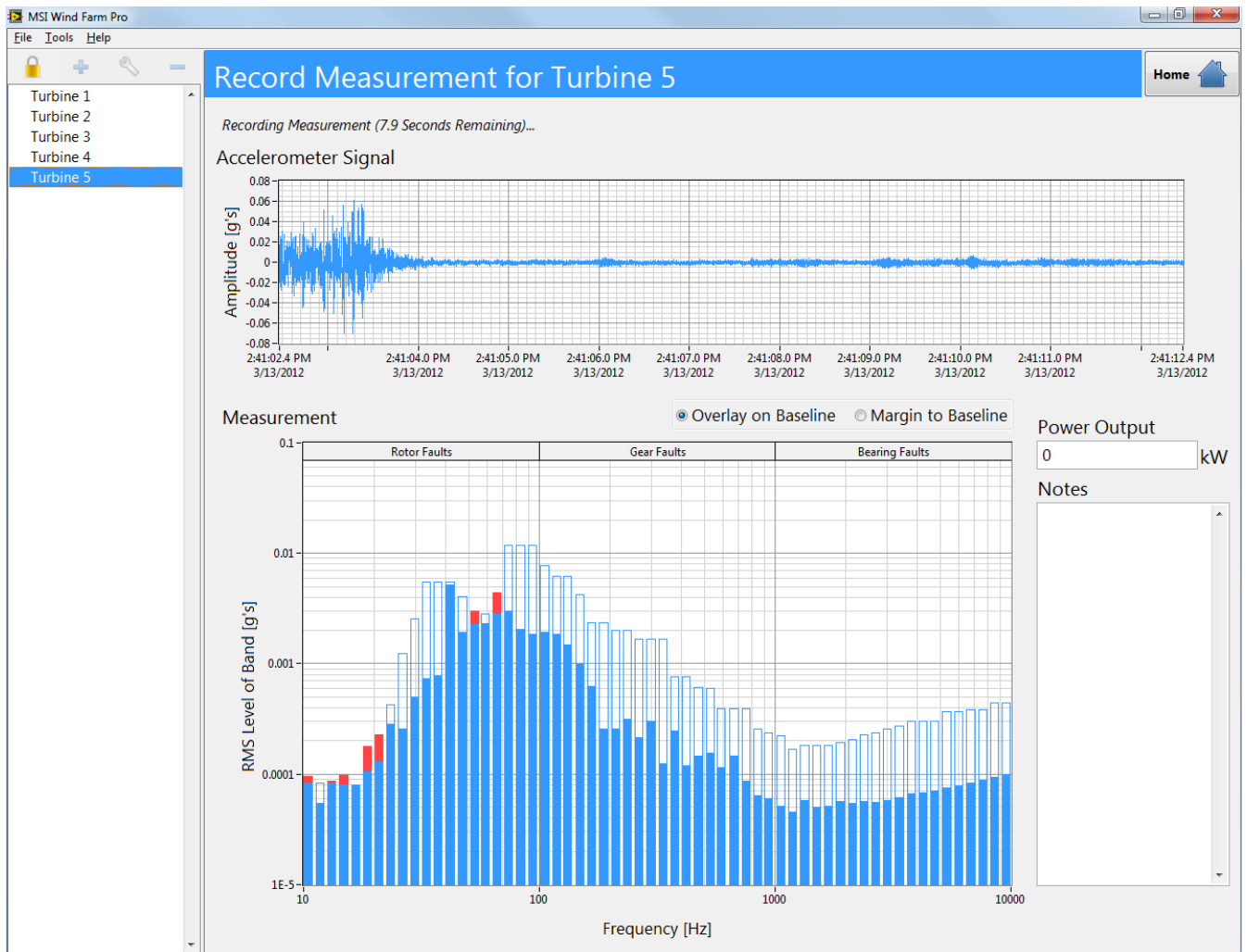


Figure 5-5. Recording a measurement. Transparent bars are baseline values; solid bars are current measurement and turn from blue to red for sectors that exceed the baseline.

Trending Turbine Health

The software provides a convenient means to compare prior measurements and to track vibration changes over time, see Figure 5-6. The top portion relates a health trend based on overall vibration level, shown as three curves plotted vs. the dates data was collected: rotor margin to baseline, gear margin to baseline, and bearing margin to baseline. For a degrading turbine, one or more curves should trend downward, eventually crossing the red colored line at zero margin. The user can move the vertical cursor through time and see, in the lower portion of the Figure, the specific CPB spectra that generated the associated data point on the trend curves. As the amount of data for a specific turbine grows over time, the user can elect which portions and baselines to show on the trend and spectrum curves.

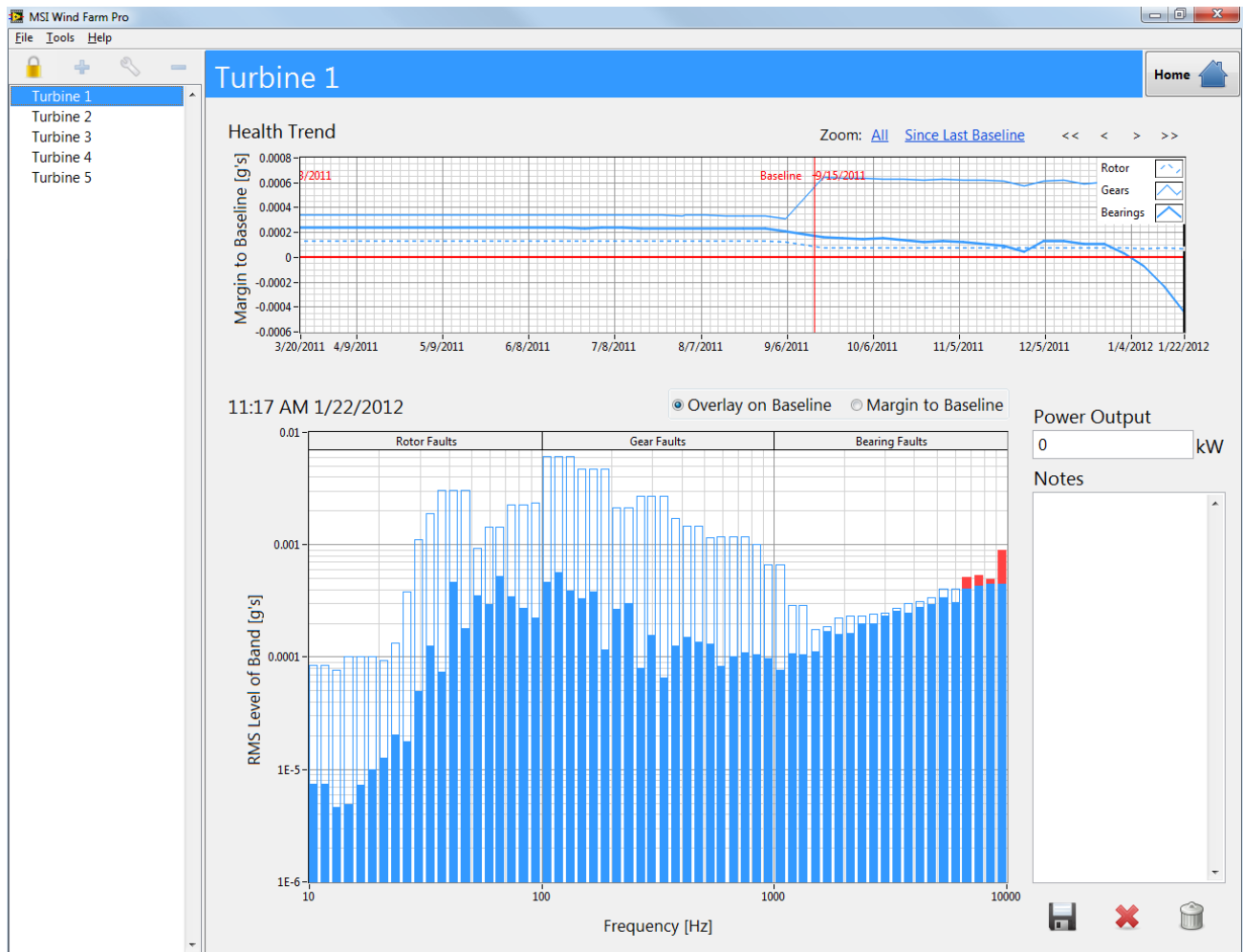


Figure 5-6. Trending turbine health. The upper portion shows a comparison to baseline over time, based on overall vibration. The cursor can be slid to a specific date. The lower portion shows the vibration spectrum for that date and time.

Advanced Bearing Diagnostics

For the user who has familiarity with spectral analysis and who has provided the system with bearing dimension information, the software provides this function to help diagnose bearing faults. This portion of the software requires user interaction and some judgment. A decreasing margin to baseline in the bearing region of the CPB spectrum may prompt the user to search for bearing faults using this feature. These faults include inner and outer race defects, cage defects, and rolling element defects. A defect is anything that prevents smooth relative motion between the bearing components, such as a crack or a spall.

Positive identification of a bearing fault is achieved through a multi-step process, illustrated at the top of Figure 5-7:

1. Select a measurement to analyze
2. Phase demodulate the data to remove speed fluctuations
3. Spectrally whiten the data to de-emphasize periodic signal components, and accentuate non-periodic signal components (vibration caused by bearing defects is not periodic)
4. Identify the most impulsive frequency band of the signal (vibration caused by bearing defects is highly impulsive, as defective surfaces roll past loading zones, exciting the entire bearing structure). In Figure 5-7, this is the region with the highest amplitude (see color bar at right)
5. Amplitude demodulate the most impulse frequency band
6. Compute an FFT of the amplitude demodulated data and correlate any peaks with bearing defect frequencies (if bearing geometry is known)

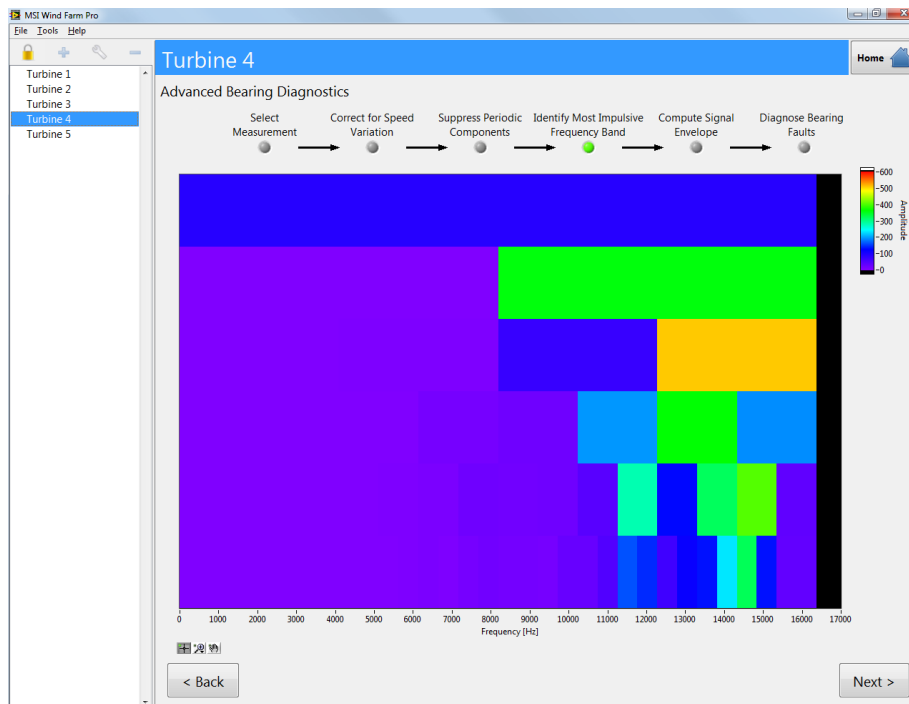


Figure 5-7. Advanced bearing diagnostics. The frequency regions with high impulse are shown in red, followed by yellow, orange, etc. as shown in the color bar on the right side of the figure.

The presence of significant peaks in the FFT of the amplitude demodulated data is indicative of a bearing fault. Even if no bearing dimension information has been provided to the system, a peak well above the noise floor is a strong indicator of a pending bearing problem. Once flagged by the MSI system, other diagnostic data, such as bearing temperatures, oil particulate counters, or vibration data collected from sensors mounted on the machinery, should be invoked. Figure 5-2 shows example FFTs for a healthy and damaged bearing. If bearing geometry information is known, the software provides cursors for each of the four defect frequencies (inner race, outer race, cage, and rolling element) for each bearing. A cursor lining up with a significant peak in the FFT represents very specific information about the type of damaged bearing component, allowing staff to address the problem before a serious failure disables the turbine.

General-Purpose Data Recorder

Finally, the software also contains a general-purpose 4-channel data recorder to enable troubleshooting measurements for further analysis with external software programs, such as LabVIEW, MATLAB, Excel, etc. For example, site staff may want to record additional, detailed vibration data on a particular turbine. In this case, the system can be placed in the nacelle to record up to four channels of data from accelerometers, proximity probes, thermocouples, or other voltage-based transducers.

HARDWARE

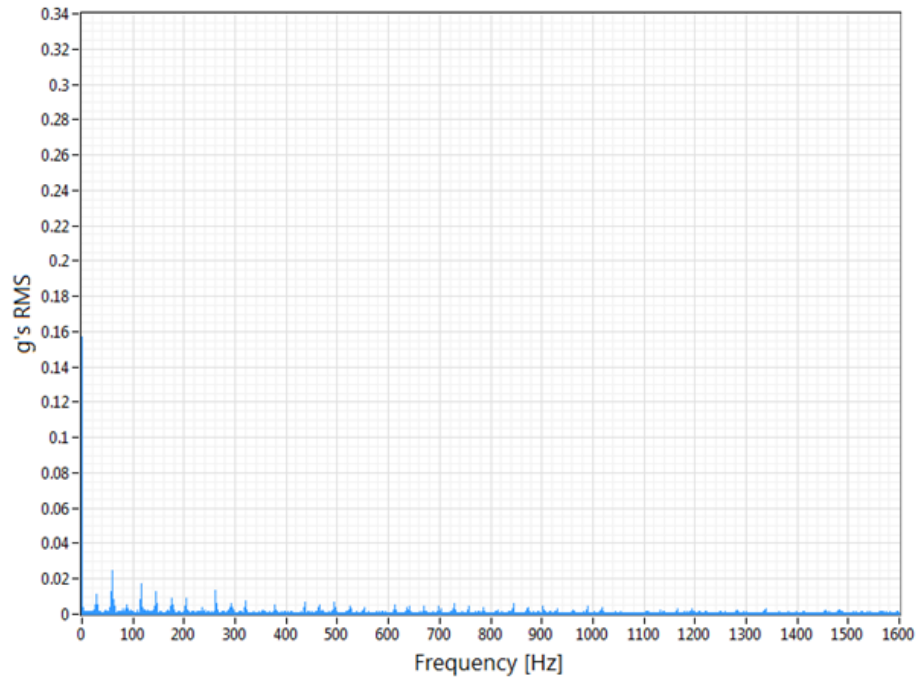
The prototype Wind Turbine Pro™ system has been implemented on the following hardware, shown in Figure S-1:

- A standard capability laptop PC, with USB 2.0 or better, running Microsoft Windows XP® or newer operating system. The laptop powers the entire system.
- A National Instruments model NI-9234 data acquisition unit. This is a USB-powered 4-input, 24-bit, 51.2 kilosamples/second device with software selectable IEPE, AC/DC coupling, and 102 dB dynamic range. A standard USB cable connects this unit to the laptop. A separate chassis: NI-cDAQ 9171 holds the data acquisition unit.
- A standard single axis accelerometer (nominal 100 mv/g sensitivity), a magnetic mount for it, and a cable to connect it to the data acquisition unit.¹⁰

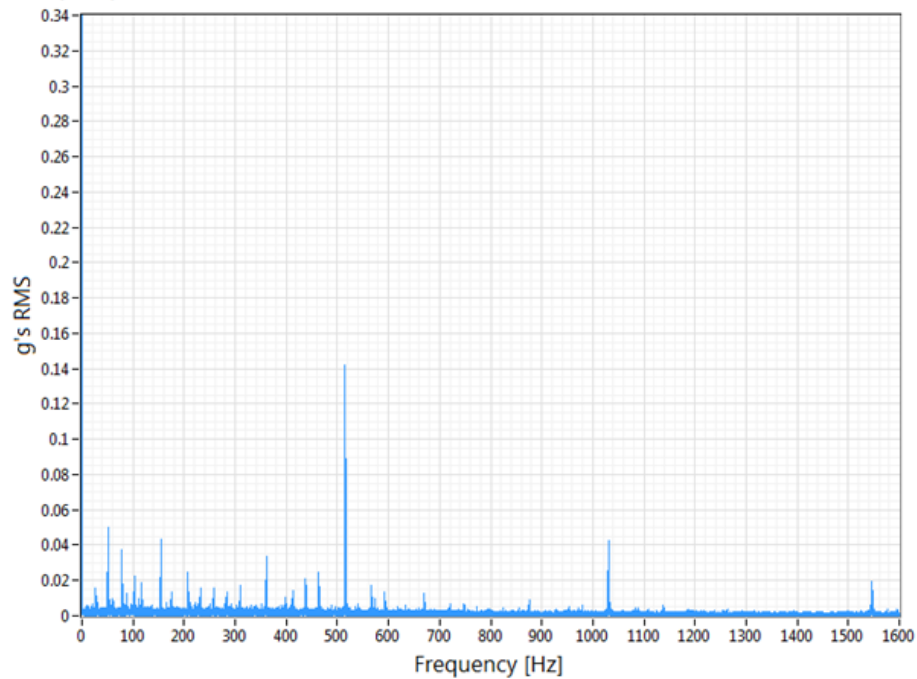
The GUI has been designed with large buttons and simple menus so it can be ported to a future tablet computer or similar device once the capability of those devices increases to the needed level.

¹⁰ For example, these items from PCB Piezotronics (Depew, NY): A model 352C33 accelerometer, a model 003C50 50 ft. long coaxial cable with 10-32 coaxial plug to BNC plug, and a model 080A27 high-strength, rare earth magnetic base with 0.75in. hex rated for 12 lbf and a 10-32 thread.

Envelope Spectrum - Measurement Mar 20, 2012 10.28.23 AM



Envelope Spectrum - Measurement Mar 20, 2012 04.29.05 PM



An

Figure 5-2. FFT of amplitude demodulated data for a healthy bearing (top) and damaged bearing (bottom). If the user provides bearing dimensional information, the MSI Wind Turbine Pro™ system can relate peaks to faulty components (inner race, outer race, rolling elements, cage).

STATUS AND FUTURE WORK

A first prototype system, embodying the software attributes and hardware items¹¹ discussed above has been assembled and tested in-house. At the time this report was prepared, the prototype system had been demonstrated to several wind farm operators, and one wind turbine OEM, with good results. Details of this activity are related in Section 6, Technology Transfer.

MSI has applied for this trade mark for the system: MSI Wind Turbine Pro™.

At the present time and going forward, MSI is using internal funds to solicit potential users/evaluators for MSI Wind Farm Pro™. Specifically we are interested in beta testers who are interested in providing feedback regarding usability and suggestions for future improvement and expansion. In this regard, MSI is providing the software on a no-fee but limited-use basis. If necessary, MSI will loan the user some or all of the system hardware. As the experience base grows, MSI anticipates incorporating salient new features and upgrades.

¹¹ Regarding hardware for the first prototype system, a National Instruments Model NI-9234 data acquisition unit and a NI-cDAQ 9171 chassis were purchased using Agreement 18800 funds. As a non-deliverable item, this unit will remain with MSI for system demonstration use going forward. The remaining hardware items in the first prototype, including accelerometer, accelerometer cable, and laptop computer, were existing, MSI-owned items.

Section 6

TECHNOLOGY TRANSFER

This section summarizes MSI work to transfer the technology developed under this project. As noted below, several of these efforts were underway or just beginning, at the time this report was prepared. MSI anticipates continuing related work, using company funds, going forward.

2011 WIND TURBINE CONDITION MONITORING WORKSHOP

MSI attended the 2011 Wind Turbine Condition Monitoring Workshop hosted by the National Renewable Energy Laboratory (NREL) September 19-21, 2011. A summary of related observations from the Workshop are noted below. In conjunction with MSI's prior and subsequent project work (see Sections 2 - 5), this information supported our decision to implement the constant percentage bandwidth (CPB) spectrum, also known as a fractional octave spectrum, instead of typical analysis methods based on discrete frequency identification and tracking, as historically implemented in vibration-based machinery monitoring systems approach (see Section 5).

Workshop Summary

The workshop featured more than forty speakers from industry, government, and academia discussing various aspects of condition monitoring for wind turbines. The workshop culminated with the presentation of results from a preceding blind study in which over a dozen experts were given vibration data from a damaged wind turbine gearbox and asked to identify as many faults as possible. The experts were supplied with gearbox geometry data such as tooth counts and bearing defect frequencies, but no information on the nature or number of faults.

As described in preceding sections of this report, using vibration data to evaluate gear and bearing health is uniquely challenging for wind turbine applications. Several noteworthy points were emphasized by the various speakers at the workshop that support this assertion. This was further evidenced by the poor outcome of the blind study where most participants correctly identified only two or three gearbox faults out of seven present, with several false-positives each. Considering the meager success of this blind study in which all signal analysis was performed with an expert human in-the-loop and full access to gearbox geometry, it is apparent that there is vast room for improvement both in identifying faults and automating the signal analysis.

As stressed by the speakers, the difficulty in applying traditional FFT-based vibration analysis to wind turbine condition monitoring is exacerbated by several factors. First, even assuming a data set from constant-speed operation, there are still literally dozens of frequencies of interest in a multi-stage gearbox that could indicate gear or bearing problems. In many cases, frequencies either overlap or are so close that identifying the true source is impossible. This is all exacerbated by the extra spectral peaks that show up as sidebands from load modulations, and the smearing of peaks from speed modulations. Participants reinforced the notion that just knowing the many fault frequencies is uncommon; in most situations the gearbox and bearing geometry is proprietary to the OEM and

not easily accessed by the site operator. Attendees also stressed the further complication at the site-wide level stemming from the many possible combinations of gearboxes and generators, each with its own unique set of dozens of characteristic fault frequencies. As an example, one speaker noted that a wind farm in Oklahoma has eighty 1.5MW GE turbines that among them include three different types of gearboxes and four different types of generators. Turbine drivetrain homogeneity across a wind park is simply impractical. Thus, wind turbines have numerous caveats to consider when performing FFT analysis, in addition to more widely-mentioned speed and load variations.

Given all these challenges, the most-discussed condition monitoring approach at the Workshop did not involve vibration analysis. Rather, much of the discussed research involved monitoring for statistically significant differences between predicted and measured temperatures at key points throughout the wind turbine drivetrain. Input variables including load, speed, ambient temperature, and their recent histories, are being used to compute the expected local temperature of things such as bearing housings. A combination of a physics-based and statistics-based approach is used to compute the expected quantities, though presenters did not elaborate further. While this method has its role, diagnostics based on temperature will always lack specificity, and requires either or both physics-based modeling and statistics-based modeling. Physics-based modeling requires machinery information that may not always be available while statistics-based modeling requires baseline data or a “learning” period.

Workshop-Based Findings

A key Workshop take-away was reinforcement of the notion that MSI’s vibration-based approach should not depend on FFT analysis was valid and strongly worth pursuing, and could provide significant value-added information to site operators. As one speaker pointed out, it’s rather straightforward for even someone untrained in vibration analysis to correctly identify a problem spectrum from among several FFTs, based on which has the noisiest and most disparate peaks. While it may remain elusive for vibration techniques to identify the exact location and severity of faults within a nacelle, it is still possible to qualify general bearing and gear health, with the possibility of providing more specific information when gear and bearing geometry is available. As expressed by wind farm operators to MSI, this type of information will be valuable in planning and organizing maintenance schedules given the finite availability of manpower and other resources. Overall, the Workshop provided valuable input for the approach MSI has implemented in this NYSERDA project.

2012 AWEA WINDPOWER CONFERENCE AND EXHIBITION

The MSI program manager participated in the American Wind Energy Association (AWEA) Windpower 2012 Conference and Exposition, June 3-6, 2012, in Atlanta. A poster (see Appendix C) summarizing the work accomplished in this project was prepared and presented. The poster was on display in the exhibition hall throughout the conference, and many hard copies were picked up by passersby. Several contacts with good potential were made or reinforced via sidebar discussions throughout the conference and during the formal poster presentation session, including:

- J. P. Morgan Capital: Several J. P. Morgan clients are interested in pro-active Operations & Maintenance (O&M).
- GE Power & Water: As a leading US-based wind turbine supplier, GE should have significant interest in our work.
- Massachusetts Military Reservation at Otis Air National Guard Base, Cape Cod, MA: They recently installed two 1.5 MW wind turbines and have a third, older unit. All are being used to power the base's push to remediate contaminated soil and groundwater using green power. There is an O&M group there that may be interested.
- The AWEA Condition Based Maintenance (CBM) Working Group is developing an O&M manual of recommended best practices, and is looking for help.

Follow up with each of the above is underway, with the most significant items to date noted below.

INTERACTION WITH WIND TURBINE OPERATORS

The following summarizes principal connections with several regional wind farm operators during this project. As related elsewhere in this report, these interactions provided important input to the work conducted. MSI anticipates continued dialog with these operators going forward.

EDP Renováveis

Based in Portugal, EDP-R owns more than 2,100 wind turbines in the U.S., including nearly 200 that produce 320+ MW at the Maple Ridge wind farm in Lowville, NY.¹² MSI initially visited the Maple Ridge site in April 2011 to describe planned project activity and solicit interest in our work. The turbines there are Vestas (Danish) model V82, installed in 2005. They are under extended warranty through 2016.

EDP-R staff saw the MSI poster (see Appendix C) at the June 2012 Windpower Conference. As a result MSI revisited the Maple Ridge site in July 2012 and demonstrated the prototype MSI Wind Turbine Pro™ system to the Operations Manager and others. Site staff was very receptive to the notion of beta testing for us, taking the measurements themselves if MSI loans them equipment, or allowing MSI site access to collect data. Maple Ridge also volunteered one or more of their turbines for future testing, if the need arises. Additional follow-up is underway.

¹² EDPR entered the U.S. market in 2007 with the acquisition of Horizon Wind Energy LLC from Goldman Sachs. The addition of Horizon, now EDPR North America (EDPR NA), helped to more than double EDP's wind-power production, making it one of the world's largest producers. The US developer had a large portfolio consisting of 559 MW in operating wind farms and 997 MW under construction. EDPR NA is based in Houston, Texas, and maintains offices and wind farms throughout the United States and Canada. The North American operation has seen rapid growth since 2007, operating over 3,300 MW at 28 wind farms. Source: EDP-R web site: <http://www.edpr.com/OurMarket/USA>

ENEL Green Power S.p.A.

Based in Italy, ENEL operates 682 wind farms in 11 countries.¹³ ENEL's North America operations include the Fennel Wind Farm in Cazenovia, NY. MSI visited the site in April 2011 to describe planned project activity and solicit interest in our work. The Fenner site has nineteen GE 1.5 MW wind turbines. They are more than 10 years old and out of warranty. ENEL operates another nearby wind farm that has Vestas Model V47 turbines, rated at 650kW each.

MSI re-visited the Fennel site in July 2012 and demonstrated the prototype MSI Wind Turbine Pro™ system to the Operations Supervisor and others. Site staff was very receptive to the notion of beta testing a system, taking the measurements themselves if MSI provides the equipment. Additional follow-up is underway in this regard. Fenner staff also noted that some turbines already have a PC inside the tower base, so in those cases a wind farm may be interested in having a dedicated, continuous monitor instead of a portable device. This could be a future enhancement or optional implementation of the Wind Turbine Pro™ system.

Noble Environmental Power

With Headquarters in Essex, CT, Noble was founded in 2004 and has wind farms in upstate and western New York and in north Texas.¹⁴ MSI visited Noble's Plattsburgh office in April 2011 to describe planned project activity and solicit interest in our work. North Country Operations has 257 GE 1.5 MW wind turbines, spread among four separate but nearby wind parks. The units are 3-4 years old and out of warranty. Noble's VP of Operations expressed keen interest in our work and arranged for this project's initial data collection visit in May 2011, when up- and down-tower vibration and acoustic data were collected on two turbines. MSI re-visited the site in late January 2012 to collect additional data from seven turbines – one up- and down-tower during overnight operation, and six down-tower samples of 5 minutes each. Section 3 and appendices A and B relate some of the data collected during these visits.

MSI re-visited the North Country site in July 2012 and demonstrated the prototype MSI Wind Turbine Pro™ system to the engineering staff and Plant Manager. Site staff was receptive to the notion of beta testing a system, taking the measurements themselves if MSI provides the equipment. They would prefer to wait until the autumn 2012 windy season.

INTERACTION WITH A WIND TURBINE MANUFACTURER

GE Power & Water staff visited the MSI poster at the Windpower Conference. Based on this interaction and subsequent discussions, a mutual nondisclosure agreement has been signed. GE is directly purchasing a set of hardware, and MSI has loaned GE an executable version of the Wind Turbine Pro™ software. Plans are for GE to

¹³ Source: ENEL web site: <http://www.enelgreenpower.com>

¹⁴ Source: Noble web site: <http://www.noblepower.com>

use the system during an upcoming series of wind turbine tests, and provide MSI with related feedback. Separately GE may be interested in incorporating some of the MSI system's data processing algorithms into a factory-installed vibration monitoring system GE is developing for future wind turbines.

INTERACTION WITH AWS TRUEPOWER

Separately, MSI discussed with AWS Truepower their on-going NYSEERDA project to mine wind farm SCADA data. Recent discussions indicate that Truepower will likely postpone work on the planned next phase of this work – integrating their system with CBM systems like Wind Turbine Pro™ – due to resource and priority issues there. Discussions with Truepower are planned for the near future, to assess if there are ways the companies might work together in this regard.

INTERACTION WITH AWEA

The American Wind Energy Association (AWEA) has formed a Working Committee focused on Condition Based Maintenance (CBM). This group is developing an O&M manual of recommended best practices, and is looking for help. Specifically, they are developing a variety of Recommended Practices (RPs) to help wind farm operators maintain their equipment. MSI has since joined the group, and has submitted Wind Farm Pro™ as an emerging technology.

Section 7

CONCLUSIONS, RECOMMENDATIONS and FUTURE WORK

This section presents specific conclusions drawn from the work accomplished, along with related recommendations and current MSI plans for carrying the work forward.

CONCLUSIONS

Based on the work accomplished, it is concluded that:

1. There is sufficient structural vibration at the base of a wind turbine's tower to form meaningful indications of the running condition of the turbine drive train, at least to the first order.
2. Properly configured, a single industry-standard vibration sensor (an accelerometer) can detect this information. A standard magnetic base can be used to attach the sensor to the tower.
3. A commercially available data acquisition device can, through a single cable, power the sensor and receive and process its signal.
4. A standard laptop computer running Microsoft Windows® can power the entire system and, with custom software developed under this project, collect, process and store relevant data and present it to the user in a logical and easy- to-understand way.
5. This combination of laptop-powered items results in MSI Wind Turbine Pro™, the industry's first easy-to-use, portable, noninvasive wind turbine machinery condition assessment system. A prototype system has been built, tested, and demonstrated to potential users. Initial feedback has been positive.

RECOMMENDATIONS

Based on these conclusions, it is recommended that:

1. The system be thoroughly tested by interested wind farm operators, with results fed back to verify, expand and upgrade the system hardware and software.
2. Work be continued to assess the role for a single ground-based acoustic sensor (a microphone) as a potential means to detect wind turbine machinery degradation.
3. The system be ported to a tablet or similar electronic device, once the capabilities of those products advances to the degree needed.
4. Consideration be given to adapting the monitoring system to use an existing PC inside the tower base for those turbines that have them. Properly configured, this could allow for continuous monitoring and dedicated sensors, with data transmitted to a wind farm's central office.
5. A working relationship be developed with nearby AWS Truepower LLC regarding combining their NYSERDA co-funded work to mine wind turbine SCADA data for improved operations with the benefits of an effective CBM system like Wind Turbine Pro™.
6. A working relationship be developed with one or more wind turbine providers, as a means of: A) further expanding the use of Wind Turbine Pro™, and/or B) extrapolating the data collection or analysis methods

assessed in this project to a provider-installed condition monitoring system for back fit and for new wind turbines going forward.

7. Participation in the AWEA CBM Working Group be continued, as a means to foster a presence in this community and contribute to the advancement and application of related practices and methods.
8. Additional avenues to present the results of work accomplished and to solicit additional interest and use be undertaken. Paths include technical papers, magazine articles, related symposia and workshops, etc.
9. NYSERDA fund additional work to further the development and application of the technology begun in this project.

ON-GOING and PLANNED WORK

Within the confines of available internal funding, MSI is proceeding with many of the recommendations cited above. This work includes purchasing, at MSI expense, additional sets of hardware that can be loaned to wind farm operators interested in evaluating MSI Wind Turbine Pro™ and providing feedback. Additional NYSERDA funding will allow quicker implementation of recommended work on a broader scale than MSI will be able to achieve on its own.

APPENDIX A

REPORT 1 FROM DR. RANDALL

In this report, Drs. Randall and Sawalhi present the notion of using frequency bands for parsing wind turbine vibration data. Applicability for this approach is principally derived from the fact that wind turbine speed can vary during light-to-medium wind conditions. The test data cited was collected by MSI during our January 31 – February 1, 2012 visit to Noble Environmental Power’s North Country site near Plattsburgh, NY.

Report to Mechanical Solutions Inc. on analysis of vibration signals measured on wind turbines, both up-tower and at tower base – Report 1 - Generation of reference spectra

by R.B. Randall and N. Sawalhi

This report is one of a number on our analysis of signals measured by Mechanical Solutions Inc. on wind turbines in operation. This report is particularly concerned with the generation of reference spectra which might be used to detect automatically if significant changes have occurred in the condition of wind turbines, using measurements made only at the base of the tower. The measurement results presented here are all from the measurements made simultaneously at the tower base and up-tower on the gearbox (specifically at point “Gearbox 3rd stage”), on Tower E-49, in January 2012.

Initial analysis shows that the signals measured at the base of the doubly-fed induction generators studied in this case contain much less information about the vibrations of the up-tower machinery than the earlier measurements, which were the subject of our preliminary report in November 2009. It is almost certain that those measurements were made on a turbine with a squirrel cage induction generator, and thus at almost constant speed, just over 30 Hz, the synchronous speed for 4-pole operation. It was found possible to locate vibration components almost certainly corresponding to the generator speed, and its 19th harmonic, supposed to be the mesh frequency of the high speed pinion. This mesh frequency could be used as a “Pseudo encoder” signal to enable order tracking of the gearbox signals and resampling in the rotation angle domain.

At this stage with the new recordings, it is difficult to locate such definite signals related to generator speed, although there is at least one just below 100 Hz, which is possibly the fourth harmonic of the planetary mesh frequency, or the mesh frequency of the pinion on the intermediate shaft. This should be elucidated in a later report on detailed analysis of the up-tower and down-tower measurements.

As suggested by Bob Randall (RBR) during his visit to MSI on 2-4 February, 2012, a simple way of comparing vibration signals over a broad frequency range, so as to detect changes in condition wherever they should manifest themselves, is based on constant percentage bandwidth (CPB), also known as 1/nth octave, spectra. This procedure is described in RBR’s book “Vibration-based Condition Monitoring: Industrial, Aerospace and Automotive Applications” (Wiley 2011) in Chapter 4. When the machine speed for a particular recording does not vary by more than about 2%, a bandwidth of 4-6% (1/18th – 1/12th octave) is recommended, though compensation can be made for larger speed differences between recordings. In the current case, where speed variations of 20-30% are possible, even in one recording, it is suggested that 1/3rd octave (23%) might be more appropriate.

The CPB spectrum comparison method has several advantages, the principal one being that it can cover a wide frequency range of three decades or more, something which is not possible with FFT spectra. Another very important one is that the effect of speed variations on dominant harmonic components in the spectrum (eg shaft harmonics, gearmesh harmonics) can be compensated by a lateral shift of the spectrum (or within the filter bandwidth if this is broad such as 1/3rd octave).

In well controlled situations where one has access to speed information of the machine (or can derive it from the signal itself) the narrower bandwidth is recommended, and a method

for generating a reference spectrum from a single measurement is suggested. This consists in smearing the spectrum one step to each side to remove sensitivity to the sampling of spectral peaks along their steep flanks, and also account for small speed variations less than the bandwidth.

Another way of generating reference spectra is to take the upper envelope of all measurements over a period where the machine is thought to be in good condition, and this is recommended here. It avoids the need to use smearing, and would not be very sensitive to changes in speed slightly greater than the filter bandwidth. Since vibrations (such as gearmesh frequencies) are often sensitive to load, it would mean that the spectrum comparison might not detect a significant change in condition until a range of loads had been encountered, but it is thought that this might be only be a matter of days or weeks as compared with the current practice of taking oil samples at intervals of six months or so. Once a change had been detected on a particular machine, new measurements could be scheduled more frequently, this being much simpler at the base of the tower.

A way of estimating $1/n^{\text{th}}$ octave spectra over three decades in frequency from three FFT spectra is described in the above-mentioned book, but it can also be done using recursive digital filters. The spectra given in this report were calculated using the Matlab program THOC, of which a copy was left with Jeremy Weiss during RBR's visit in February. The program asks the user to specify a top centre frequency (sufficiently below the Nyquist frequency that the upper frequency limit of the highest band is below the lowpass filter cutoff), as well as the number of filters. The results in this report used an upper frequency of 12.5 kHz, and thirty $1/3^{\text{rd}}$ octave filters covering three decades in frequency. The filters are genuinely $1/3^{\text{rd}}$ octave, but can be taken as having centre frequencies according to the standard acoustic $1/3^{\text{rd}}$ octave filters (actually $1/10^{\text{th}}$ decade) in the sequence: (16, 20, 25, 31.5, 40, 50, 63, 80, 100, 125, 160, ... 1.6 k, 2 k, 2.5 k, 3.15 k, 4 k, 5 k, 6.3 k, 8k, 10 k, 12.5 kHz). The difference is only 2.4% at the lowest frequency. Unfortunately, a way has not been found to scale the x-axis of the plots in this report in terms of these frequencies, so they are given just as filter number from 1 to 30.

An attempt was first made to see how much variation there was between the different sections of a typical recording of 5 mins length. Figure 2 shows the five $1/3^{\text{rd}}$ octave spectra corresponding to each minute of the recording made on the actual gearbox (GB 3^{rd} Stage). The corresponding time records of the first three minutes are shown in Appendix A, Fig. A1, which shows that the local RMS value of the signal changed appreciably over this period.

Figure 2 shows that the $1/3^{\text{rd}}$ octave spectra are reasonably repeatable, with maximum variation about 2-3 dB.

Figure 3 shows the same representation of the signals measured at the tower base over the same time period. The corresponding time signals for the first three minutes are shown in Fig. A2 of Appendix A.

It is evident that the signals measured at the tower base are noisier, as the variation is now up to about 10 dB, though mainly for filter 8 (80 Hz) and for the three highest filters (8-12.5 kHz). It is also very clear that there is a high attenuation of high frequency components, which will make it more difficult to detect bearing faults, but it should be possible.

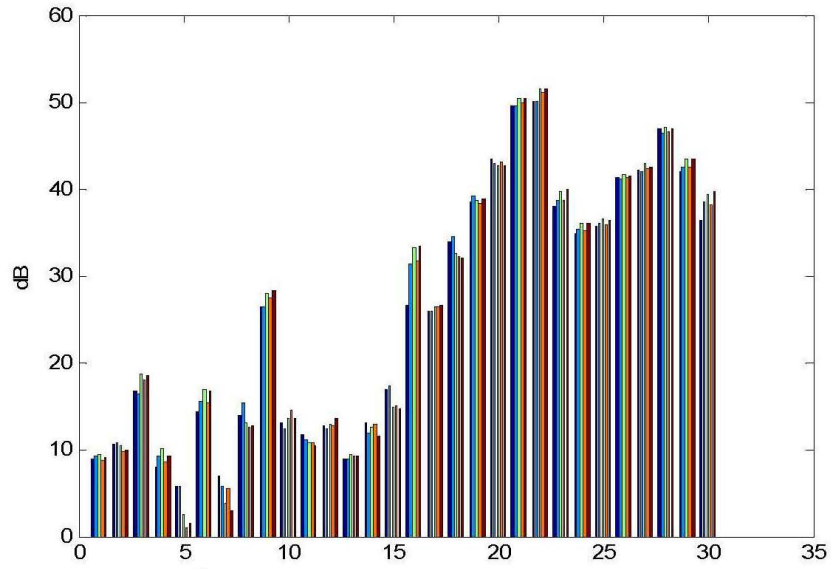


Figure 2 1/3rd octave spectra for each minute of the 5 minute recording made on GB 3rd Stage

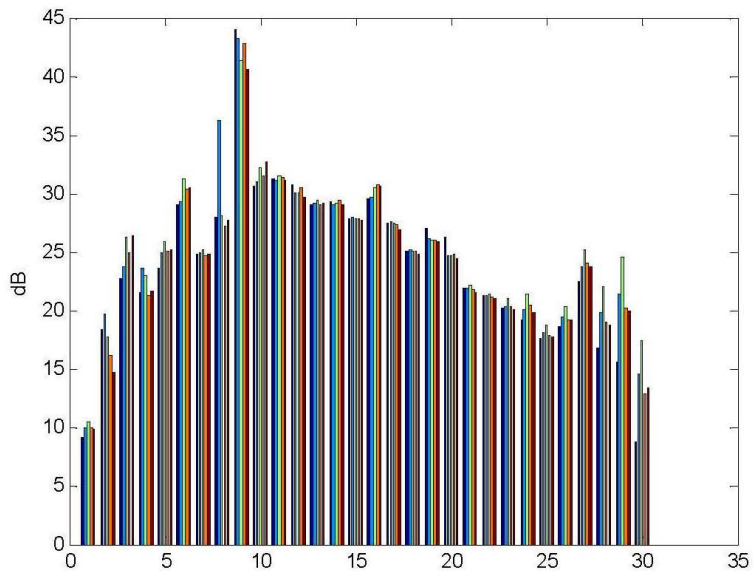


Figure 2 1/3rd octave spectra for each minute of the 5 minute recording made at Tower base

When the FFT spectra of the tower base signals were examined, there were found to be groups of evenly spaced spectral components throughout the spectrum. The spacing was measured to be 120 Hz, and they thus obviously had an electrical origin. No such components were found in measurements made on the machine, so it appears that they originate from electrical cables or other equipment near the measurement points at the base of the tower. Note that such components were not found in the earlier measurements on the squirrel cage machine, so it seems likely that they come from the speed control system associated with the doubly fed generator.

Using a harmonic cursor it was quickly established that the spectral components were not harmonics of 120 Hz, but groups of sidebands spaced at twice line frequency. It is not yet clear what the carrier frequencies are.

In any case it seemed that these components were unrelated to the condition of the machine, and so it would be a good idea to remove them before making spectrum comparisons. Since they are not harmonics, it is not possible to use synchronous averaging to remove them, so it was thought that it might be possible to use a cepstral technique based on removing specific families of evenly spaced spectral components using the real cepstrum. This treats only the amplitude of the spectra, but the edited spectra can be combined with the original phase to regenerate time signals. The phase of the residual signal would thus be in error at the locations of the removed components, but this has been shown to have negligible effect in many cases. Details of this technique were given in a paper presented at the MFPT conference in Virginia Beach in 2011, attended by Jeremy Weiss and Bill Marscher, but a brief explanation is given here, as well as the specific parameters required for these signals.

Figure 3 shows an example of how removal of a small number (in this case just one) of components (harmonics) in the cepstrum, corresponding to a particular spacing in the log

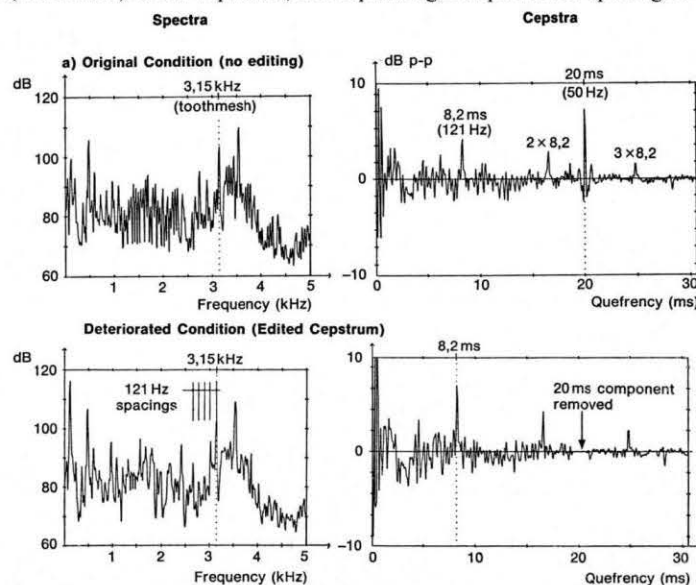


Figure 3 Example of editing in the cepstrum to remove a harmonic family

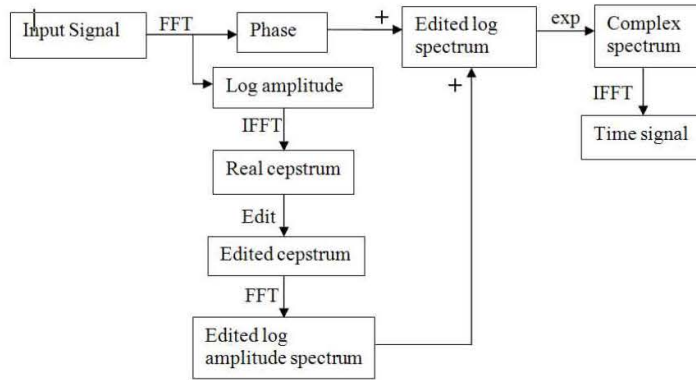


Figure 4 Producing a time signal from the edited spectrum

spectrum (harmonics or sidebands) can remove the whole family from the spectrum. When this was originally done it was not realised that it would be possible to go further than the edited spectrum, but the procedure illustrated in Fig. 4 illustrates how such an edited amplitude spectrum can be combined with the original phase to give time signals.

We have experimented with different ways to apply the “comb lifter” in the cepstrum to remove a series of harmonics. In some cases it is convenient to allow the notch to get wider for each order of harmonic, so that they eventually merge to continuous zeros and give a concurrent “lowpass lifter” which smooths the spectrum amplitudes at the same time. In this case (with the wind turbine data) this was found to change the overall scaling of the residual spectrum by a small amount (approx. 3 dB), so the alternative of a constant width notch was tried, as shown in Figure 5 (where it was combined with a “highpass lifter” that can be dispensed with in this case).

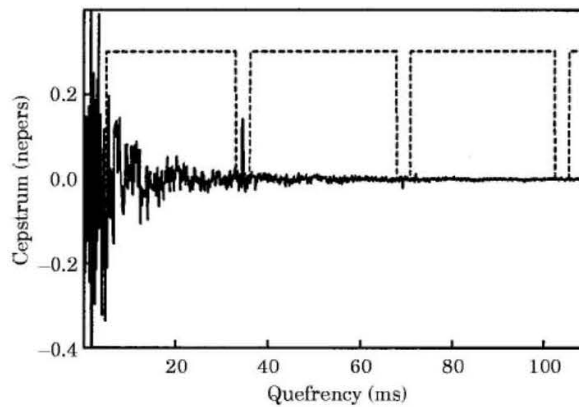


Figure 5 Illustration of a constant notch width “comb lifter”.

The former method is best when there is a random variation of the periodic length, giving a progressive smearing of higher harmonics (and rahmonics) whereas the latter is best when there is a constant frequency window causing all spectral components to be broadened by a fixed amount. This is particularly the case here, as the periodically spaced spectral

components are not uniformly spread throughout the whole spectrum, so can be considered as “windowed” in the frequency domain. It was found that to remove all traces of the 120 Hz sidebands it was necessary to use a notch width corresponding to $\pm 15\%$ of the value of the first harmonic. Incidentally, the combination of noise and the window smearing effect is so great in this case that peaks could not be found in the cepstrum, but because the spacing was known to be exactly 120 Hz, the corresponding quefrency ($1/120\text{s} = 8.333\text{ ms}$) could be calculated without further knowledge.

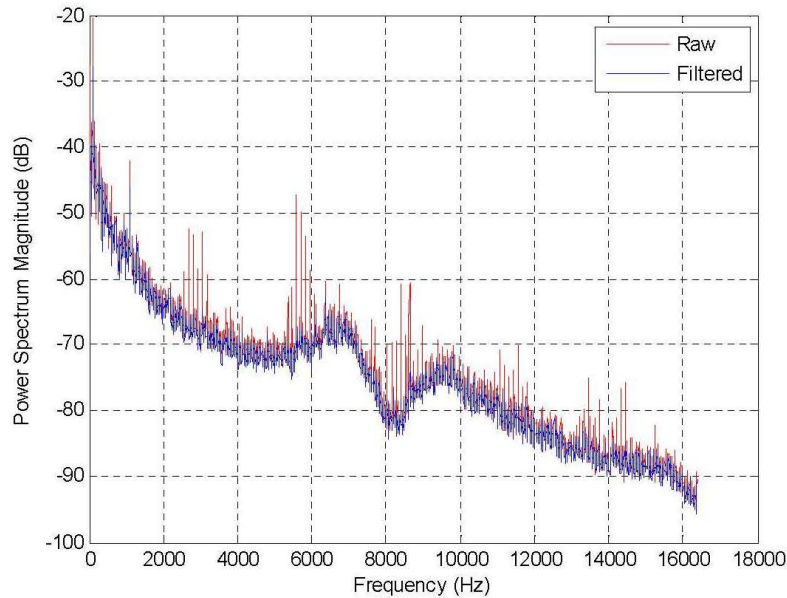


Figure 6 Spectrum of base signal with and without removal of 120 Hz components

Figure 6 shows a typical result for the FFT spectrum before and after the cepstrum editing. Because of memory problems with the Matlab calculations it was necessary to reduce the signal length processed, so the 5 min. signal was divided into eight sections each of about 37s. The one illustrated is the first, but the first five 37s sections are shown in Appendix B, after the corresponding time records before and after editing, which are added to Appendix A. It is interesting that the effect of editing appeared greater on some time records than others.

The non-edited and edited signals have been converted into $1/3^{\text{rd}}$ octave spectra, and the first five 37s sections are reproduced in Figures 7 and 8. Note that these are shorter records than in Fig. 2 (non-edited), but show about the same amount of variation, in particular in filters 8, 28, 29, 30. The effect of the filtering can be compared for the first 37s section of signal in Figure 9.

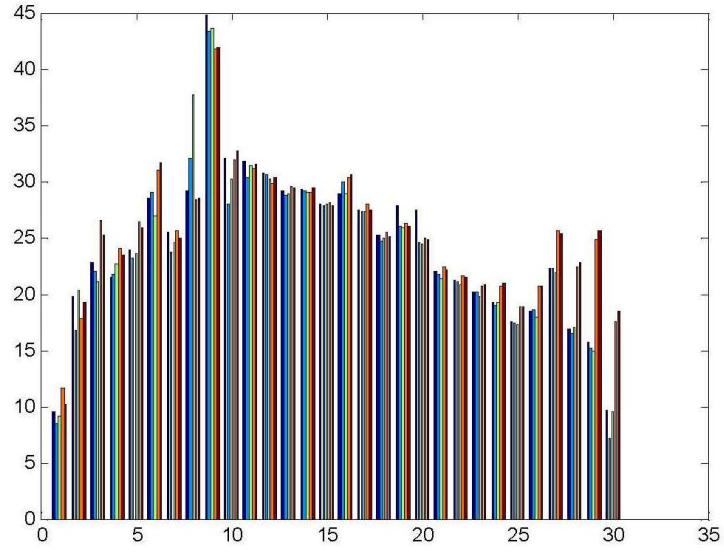


Figure 7 Similar to Fig. 2, but for the first five 37s records

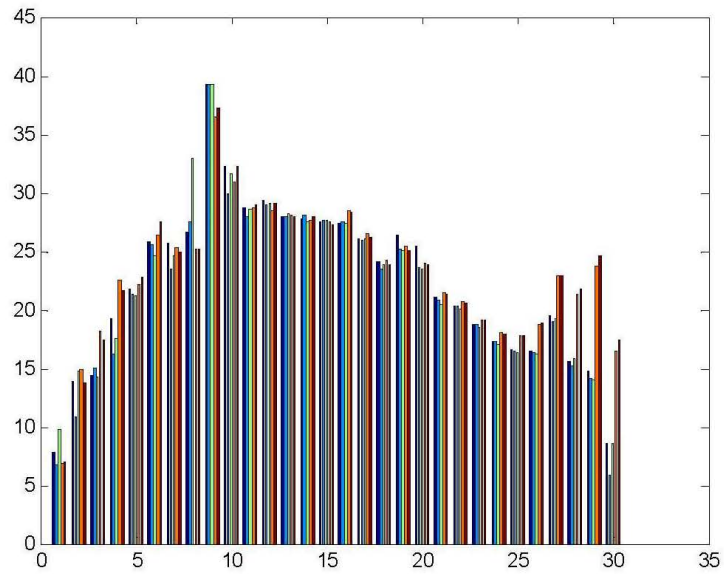


Figure 8 Similar to Fig. 7 but for the filtered data

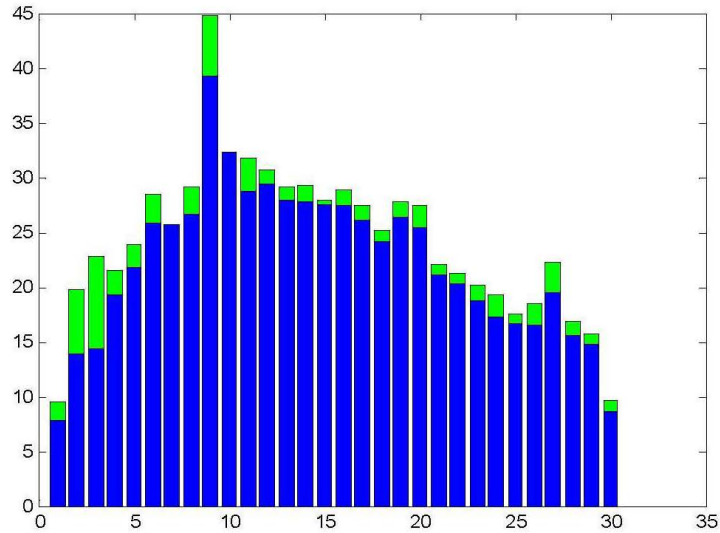


Figure 9 Filtered vs original spectra for the first 37 s.

It is interesting that there is a bigger difference (of 5-7 dB) at low frequencies than at the locations of the 120 Hz sidebands, but it is believed that this difference is a fixed effect of the filtering, and should not affect comparisons. The difference at low frequencies is not so evident in broadband spectra such as Fig. 6, but can be seen in the zoom FFT spectrum of Figure 10, which is a zoom on the low frequency part of Fig. 6.

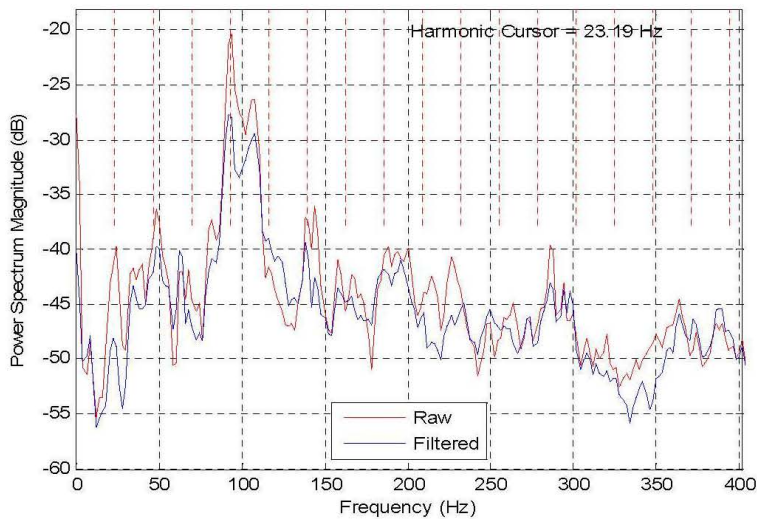


Figure 10 Zoom on low frequency part of Fig. 6.

Appendix A – Time records

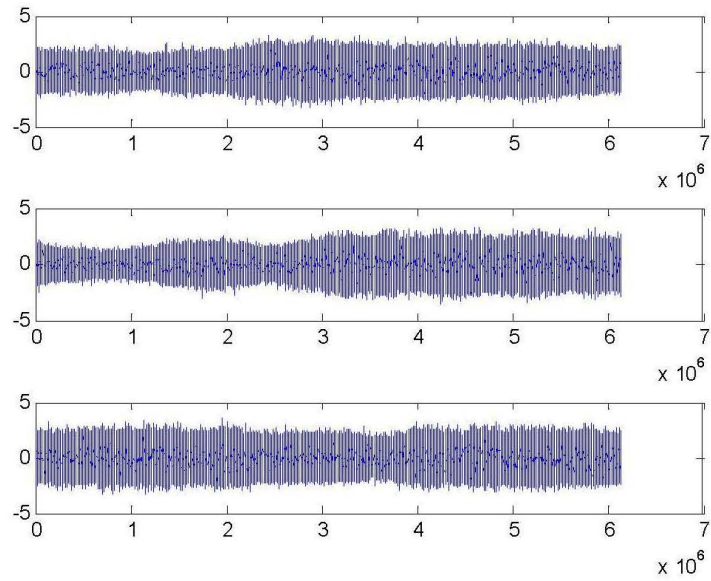


Figure A1 First three 1 min time records GB3rdSt

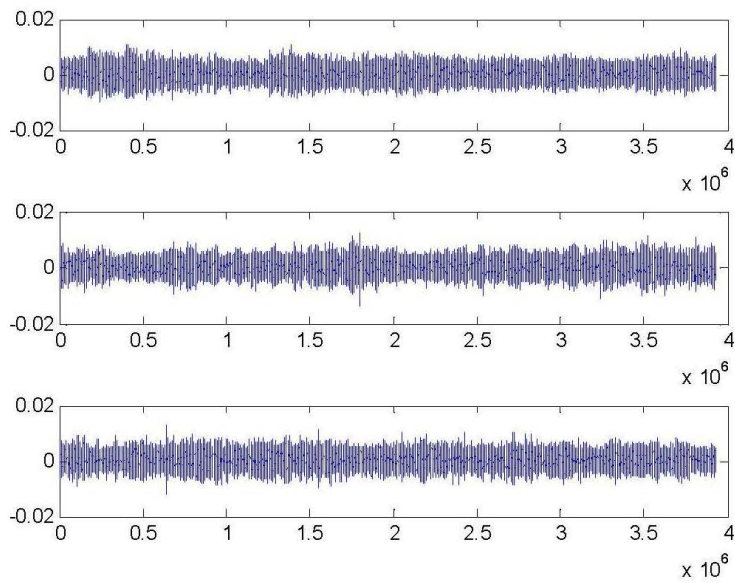


Figure A2 First three 1 min time records, Tower base, untreated.

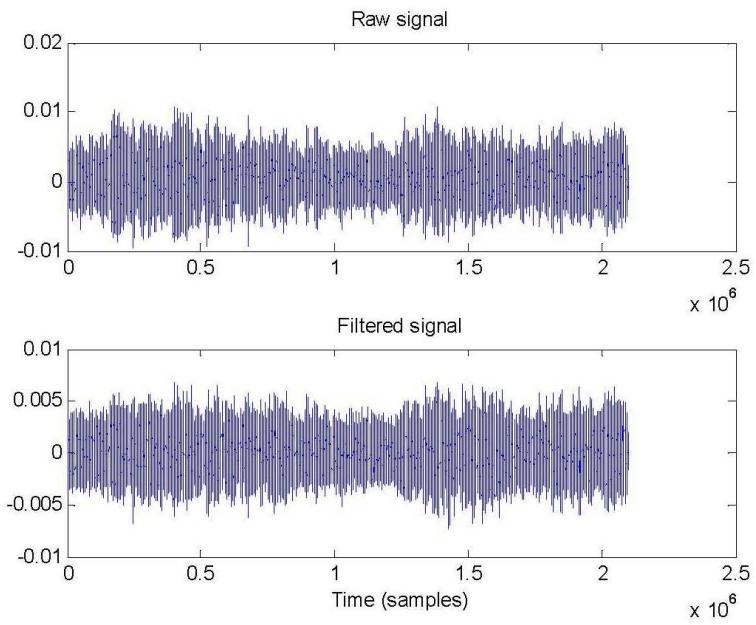


Figure A3 Filtered vs unfiltered signal for first 37s.

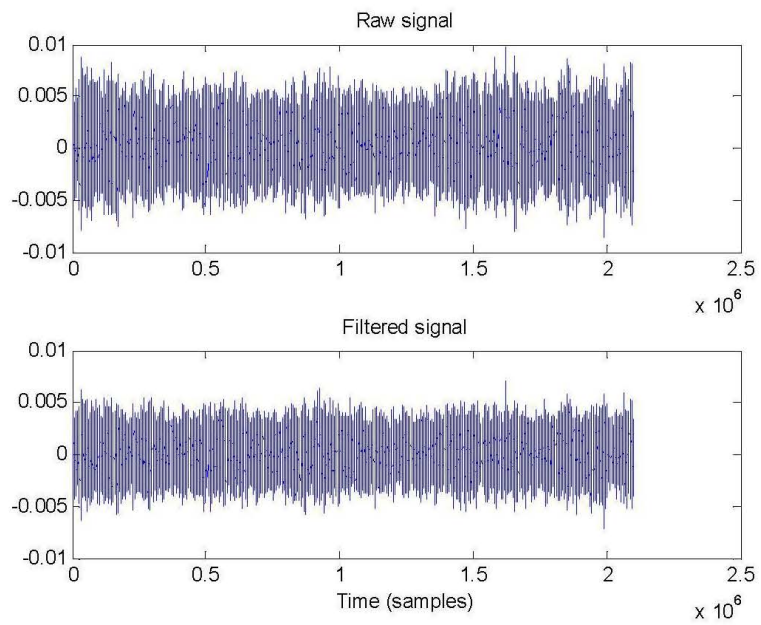


Figure A4 Filtered vs unfiltered signal for second 37s.

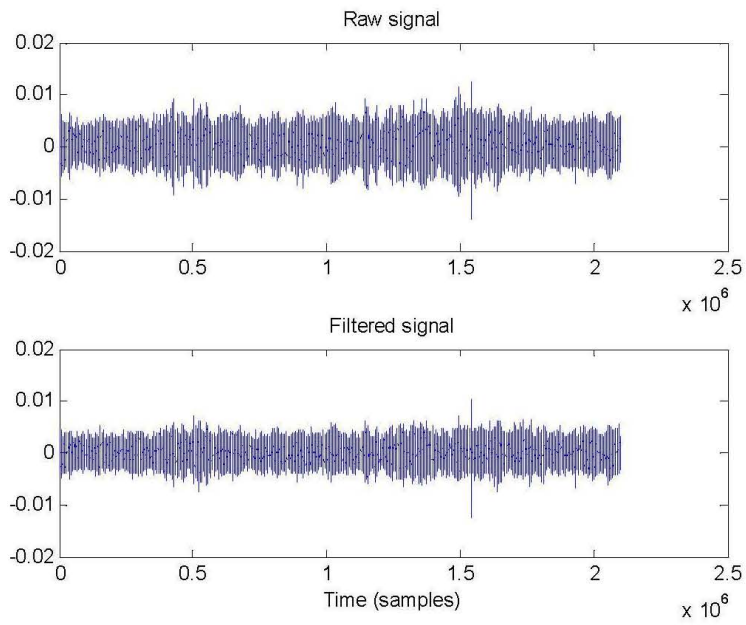


Figure A5 Filtered vs unfiltered signal for third 37s

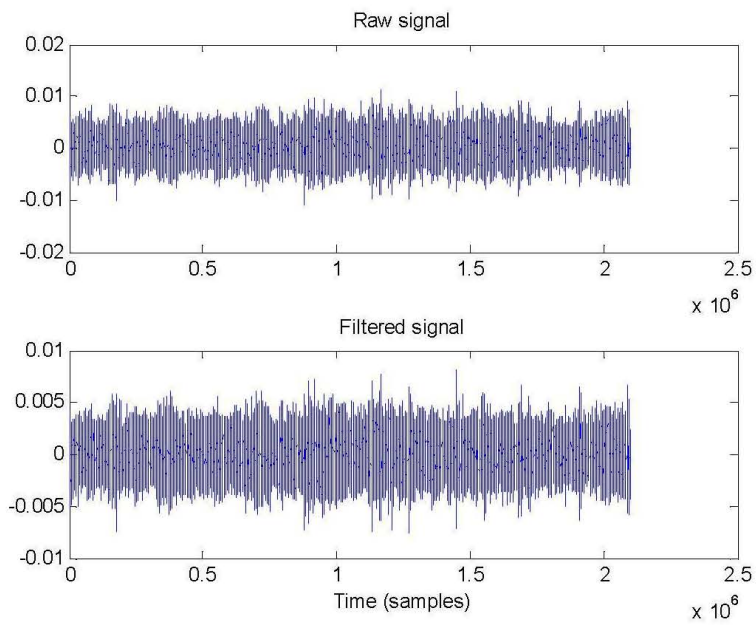


Figure A6 Filtered vs unfiltered signal for fourth 37s (Note scale)

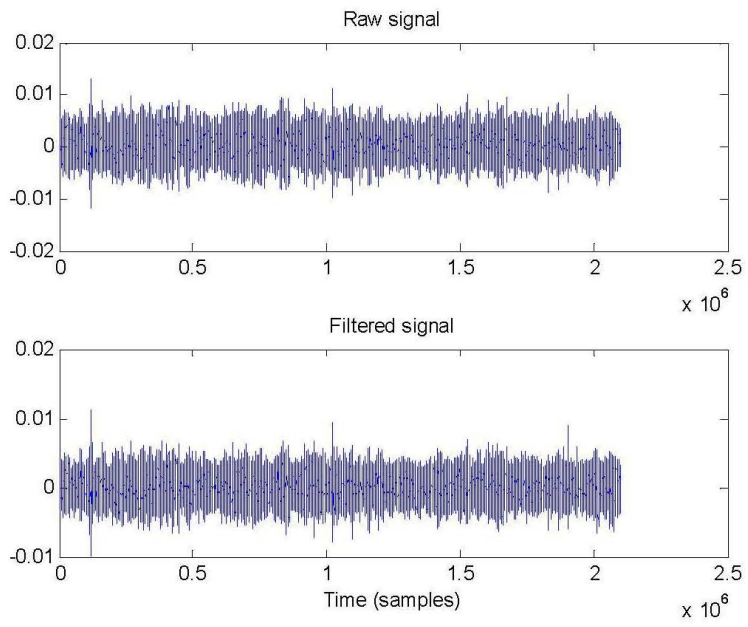


Figure A7 Filtered vs unfiltered signal for fifth 37s

Appendix B – FFT Spectra

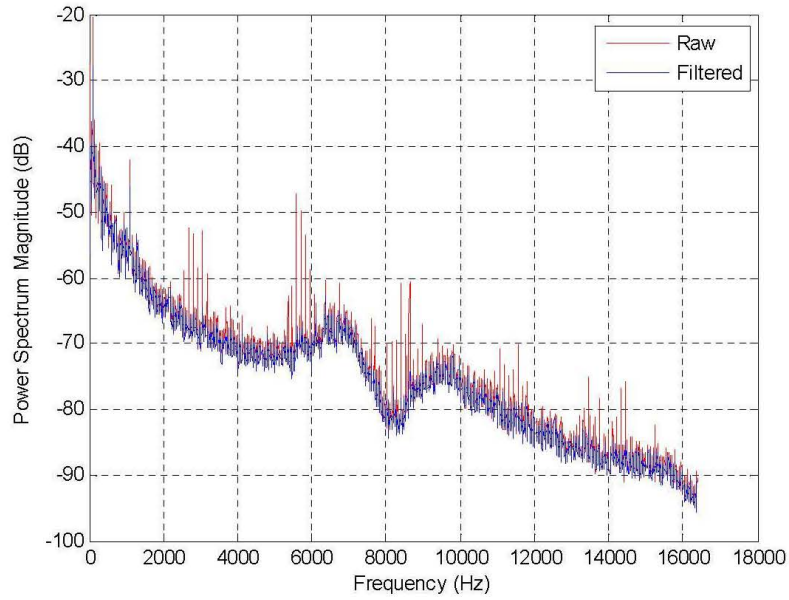


Figure B1 Spectrum editing effects, first 37s

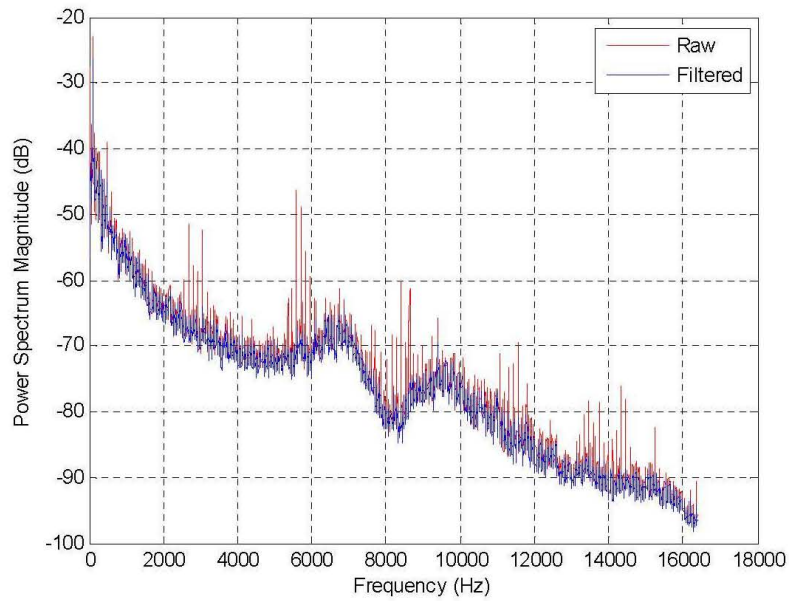


Figure B2 Spectrum editing effects, second 37s

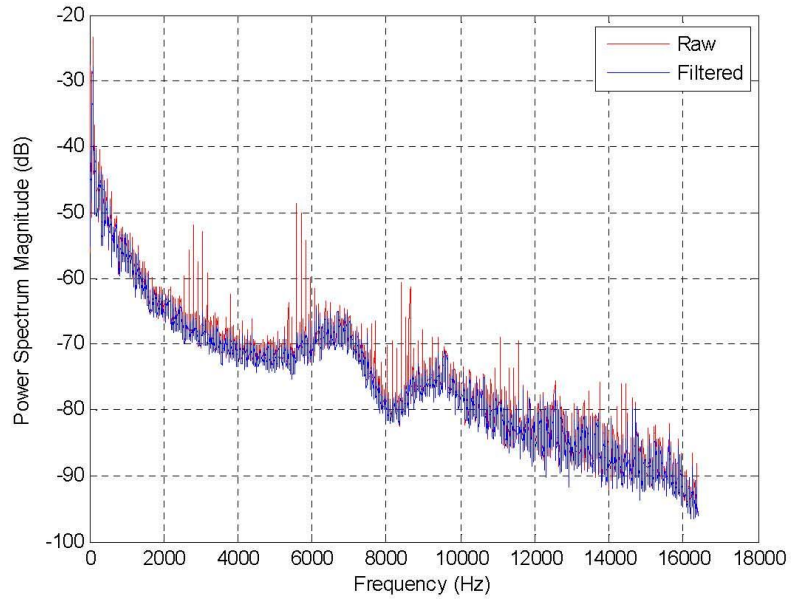


Figure B3 Spectrum editing effects, third 37s

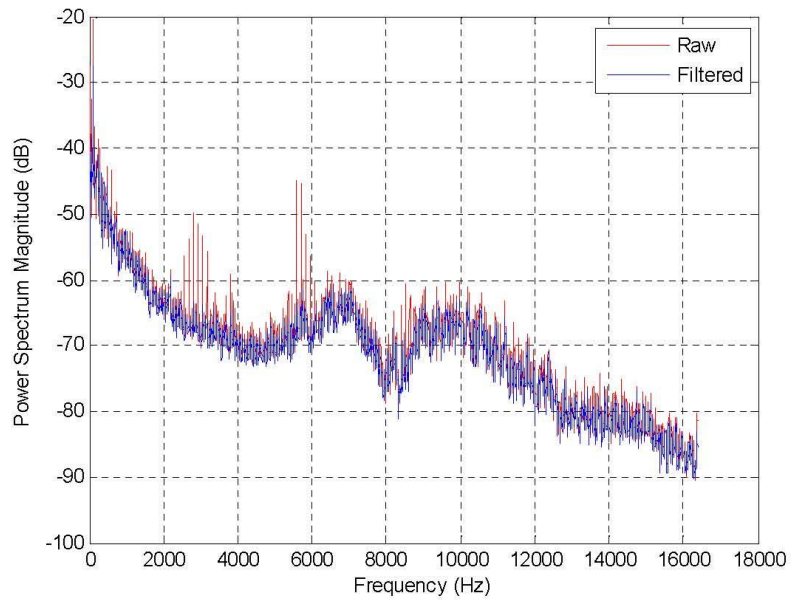


Figure B4 Spectrum editing effects, fourth 37s

APPENDIX B

REPORT 2 FROM BOB RANDALL

In this report, Drs. Randall and Sawalhi summarize their assessment of simultaneous up- and down-tower vibration measurements on an operating wind turbine. The test data cited was collected by MSI during our January 31 – February 1, 2012 visit to Noble Environmental Power’s North Country site near Plattsburgh, NY.

Report to Mechanical Solutions Inc. on analysis of vibration signals measured on wind turbines, both up-tower and at tower base

by N. Sawalhi and R.B. Randall

Report 2 - Tower E-49: Up Tower, Down Tower Preliminary Comparison and Analysis

The results presented here are taken from the “UpTower DownTower Comparison folder” mostly from the first 30 seconds of the data. The base tower data was sampled at 32768 Hz, while other data (two gearbox signals and two generator bearing signals) were sampled at 51200 Hz. Once the features and behavior are understood, further analysis will be conducted on the two other sets of the provided data. This preliminary analysis focused on analyzing the frequency content of the signals to investigate common features using both power spectral density comparisons and Short Time Fourier Transforms (Spectrograms) to extract and observe the variation of frequency content with time. This gives a very useful indication of the speed variation and was employed to verify the speed changes (profiles) obtained by signal demodulation. Successive order tracking has been attempted on the signals to remove speed fluctuations and smearing.

1. Time, Frequency and Spectrogram Comparisons

Figure 1 shows the first 30 seconds for the signal from the gearbox third stage and the one from the tower base. Note the difference in amplitude and the large variations seen in the tower base signal.

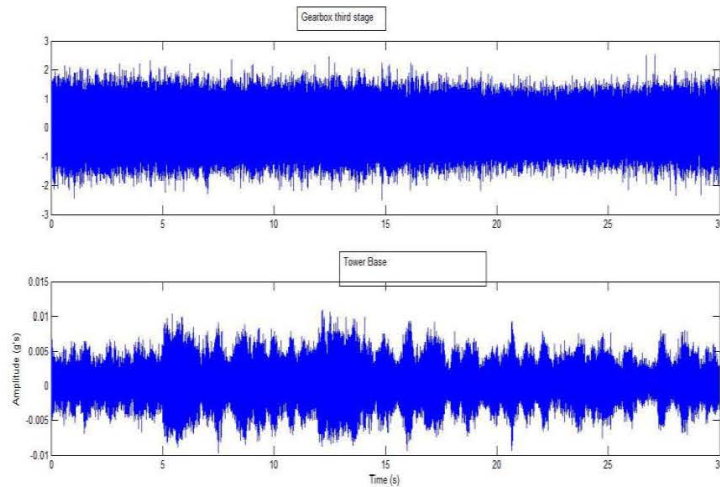


Figure 1 Time domain signals

Figure 2 shows the power spectral density (on the full available bandwidth) for the signal from the gearbox third stage and the one from the tower base. In general, measurements at the tower base share only the low frequency content (Figure 3) with the ones measured on the gearbox (i.e. the signal is low pass filtered and

attenuated as a result of the transfer path). It is clearly dominated above 2 kHz by electrical components which appear as discrete lines (sideband families at 120 Hz).

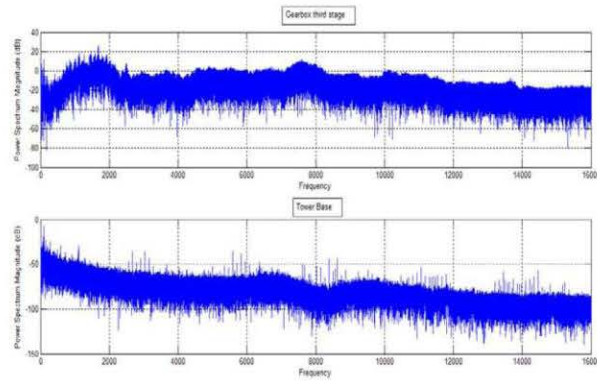


Figure 2 PSD comparisons

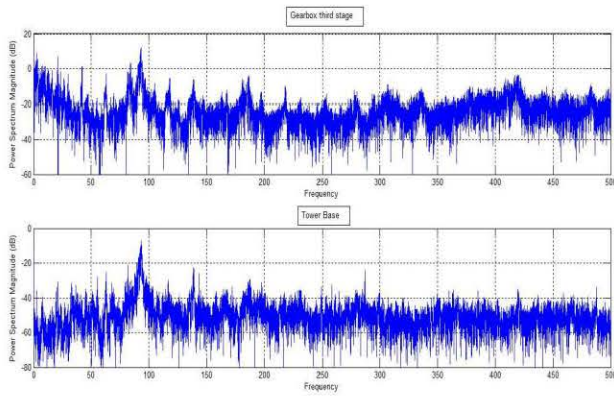


Figure 3 PSD comparisons (zoomed in: up to 500 Hz)

The spectrograms for these two signals are shown in Figure 4 and zoomed versions are shown in Figure 5. The spectrogram gives useful and interesting information about the speed changes (profiles) and indicates the presence of the highest gearmesh frequency.

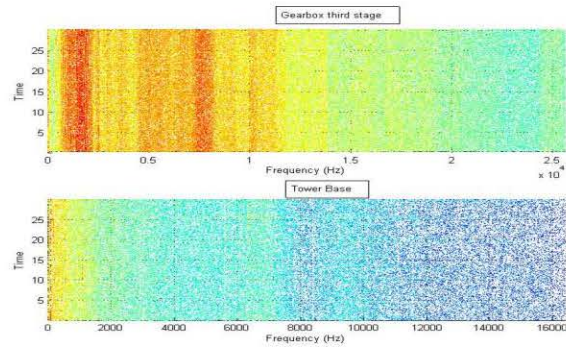


Figure 4 Spectrograms of the gearbox signal and the tower base signal

As can be seen from Figure 5, the harmonics of the HSS (high speed shaft) gearmesh frequency (around 420 Hz) are clearly visible up-tower (especially the 4th harmonic) and the speed profile can be seen very clearly and mainly from the 3rd and 4th harmonics. From the tower base data it is very difficult to get this information, but the similarities are clear in the very low frequency range, especially around 100 Hz. In another section of the data (second 30 seconds), the speed profile looks different and a trace of the high gearmesh frequency can be noticed even at the tower base, as can be seen from Figure 6.

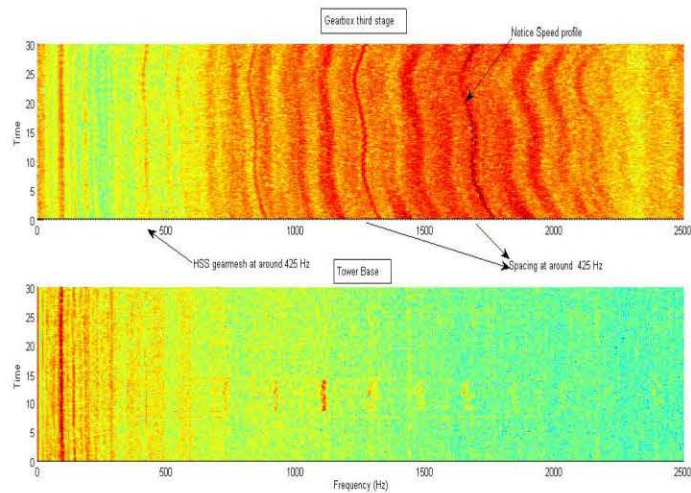


Figure 5 Zoomed-in Spectrograms

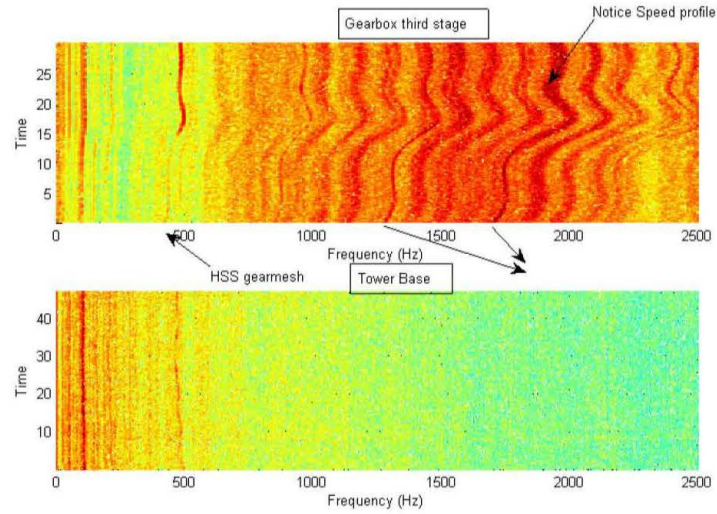


Figure 6 Zoomed-in Spectrogram (second 30 seconds of data)

The linear FFT plots around 93 Hz and 420 Hz in the first 30s are shown in Figures 7 and 8 respectively. In Figure 7, it is shown that there is a high resemblance between the signals measured from the gearbox and the ones at the tower base around 93 Hz. It is believed that this is the gearmesh of the second stage (measured from the generator) as can be seen from the attached Table 1, where gear ratios are based on the detailed analysis in Appendix A (but from a different section of signal with a different mean speed). This frequency matches very closely the supposed gearmesh frequency of the second stage.

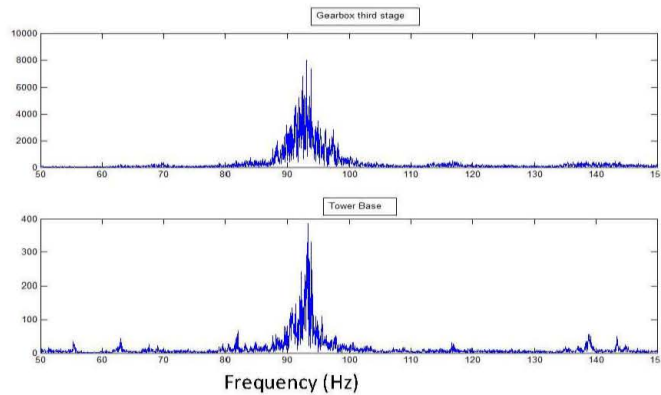


Figure 7 Linear FFT zooming around what is believed to be the gearmesh of the second stage

Table 1: Estimated shaft and gearmesh frequencies (for generator mean speed 21 Hz)

Estimated Frequencies in the gearbox

High shaft speed (Hz)		21.00	
HS-ST			HS-ST GMF
pinion	20		
gear	113		420.00
Intermediate shaft speed (sun)		3.72	
IS-ST			IS-ST GMF
pinion	25		
gear	71		92.92
Low shaft speed (sun)		1.31	
Ring gear teeth	105		Epicyclic mesh
Planet gear	39		
Sun gear	27		28.11
Out put speed (carrier)	0.268		
Planet pass frequency	0.803		
Spin frequency	-0.721		

Figure 8 compares the frequency range around the HS gearmesh from both the gearbox signal (3rd stage) and the tower signal. The gearmesh frequency around the 420 Hz component is clearly seen from the gearbox signal but is not recognizable at the tower base.

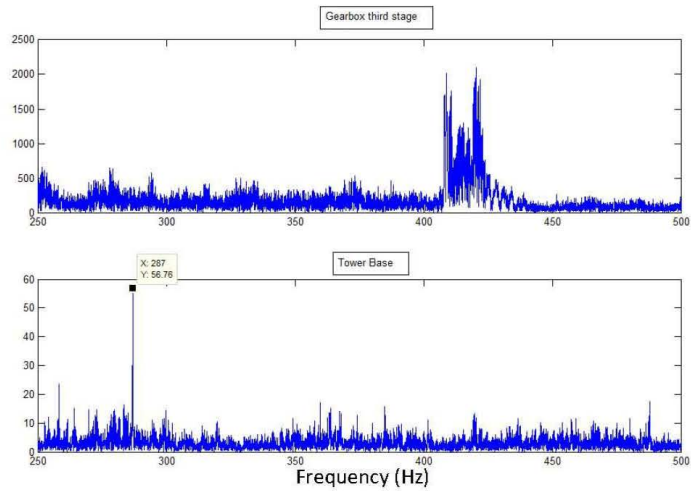


Figure 8 Linear FFT zooming around the HSS gearmesh

2. Linear FFT Comparisons around the HSS, speed profile extraction and Spectrogram Comparisons

Figure 9 shows a zoomed plot around the high speed shaft (HSS) frequency for the third stage of the gearbox and the tower base signals. Figure 10 shows a similar plot to compare the signals from the generator with the tower base, with a more similar pattern.

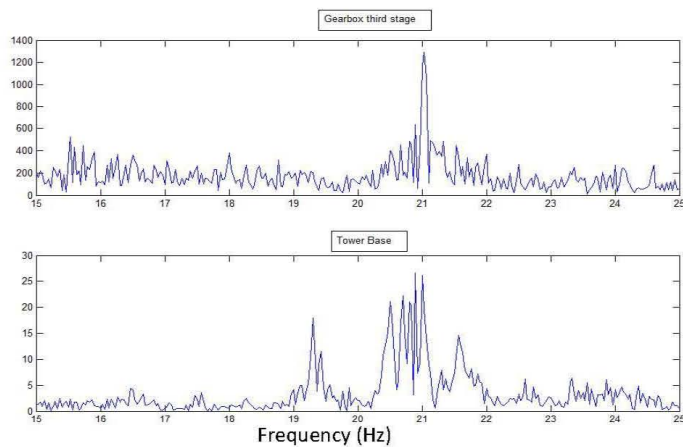


Figure 9 Linear FFT zooming around the HSS: Comparing the gearbox third stage with the tower base around 21 Hz.

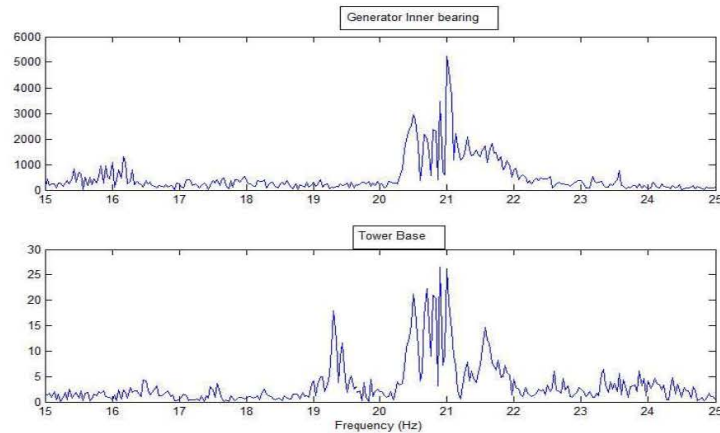


Figure 10 Linear FFT zooming around the HSS: Comparing the generator inner bearing signal with the tower base around 21 Hz.

The HSS information is clearly visible at the tower base. Phase demodulation of a band around 21 Hz was used to extract a tachometer signal for order tracking purposes. There are two ways of obtaining a speed profile. The first differentiates the demodulated phase and adds the resulting frequency variation to the carrier frequency removed in the demodulation process. The second method inverse transforms the demodulation band (without shifting it to zero frequency) and then measures the spacing between zero crossings of the modulated sinusoid (180° phase increments) and the reciprocal of these time intervals can be scaled as mean speed. Differentiation always has the potential for noise problems, and this was found to be the case here (using both methods). We are still experimenting with the best method to smooth the estimates but some results obtained by fitting a 6th order polynomial to the noisy data are given here.

The speed variation as obtained from the tower base signal and the gearbox are shown in Figures 11 and 12 and can be compared to the apparent variation obtained from the spectrograms of the gearbox signal shown in Figure 5 and Figure 13. The result obtained from the gearbox signal surprisingly has more noise problems than that from the tower base. These manifest themselves in deviations at the end of the record where the polynomial is poorly defined. It appears clearly that the information obtained from the gearbox can be generated from the tower base data.

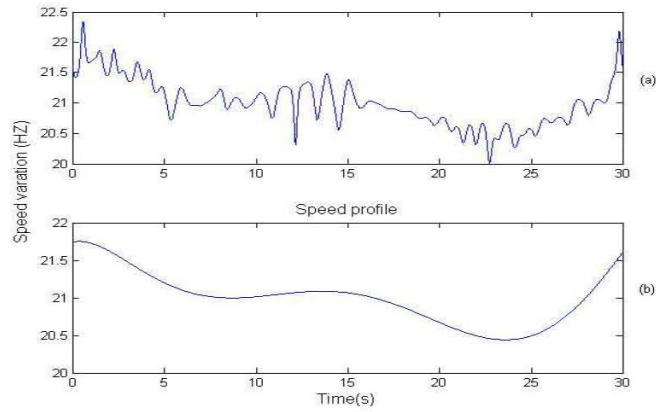


Figure 11 Speed profile obtained from HSS component measured at the tower base scaled in Hz (actual speed variation).
 (a) Lowpass filtered estimate (b) result from curve fitting a 6th order polynomial

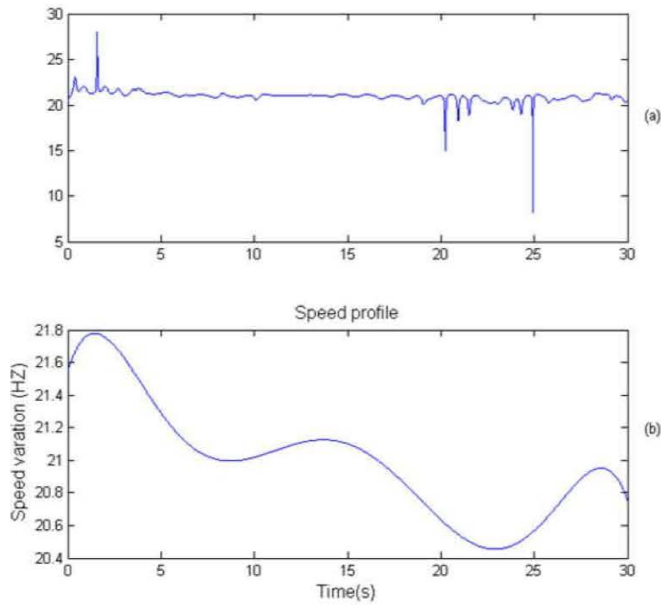


Figure 12 Speed profile obtained from HSS component measured on the gearbox scaled in Hz (actual speed variation).
 (a) Original estimate (b) result from curve fitting a 6th order polynomial

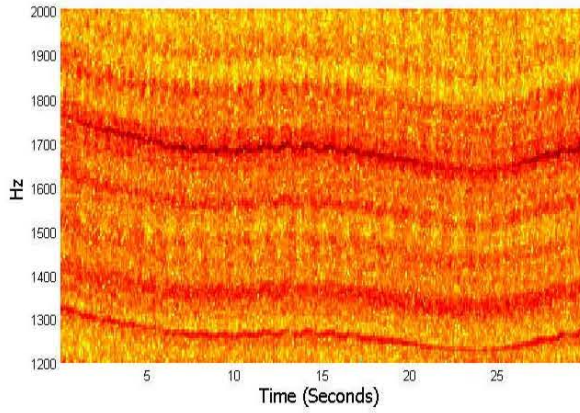


Figure 13 Spectrogram of the third stage gearbox signal. X-axis time (s). Y-axis: frequency (zoomed in between 1200 and 2000 Hz)

Figure 14 shows the speed profile estimated using the second gearmesh signal (around 93 Hz) measured on the gearbox. It has smaller end effects than that from the HSS in Fig. 11.

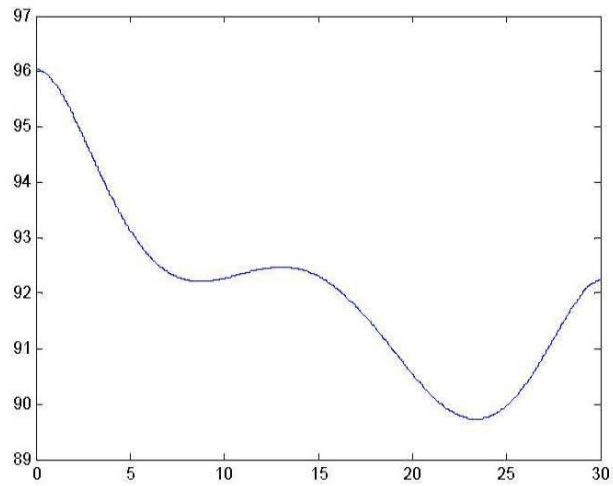


Figure 14 Speed profile obtained from 2nd gearmesh component measured on the gearbox scaled in Hz (actual speed variation).

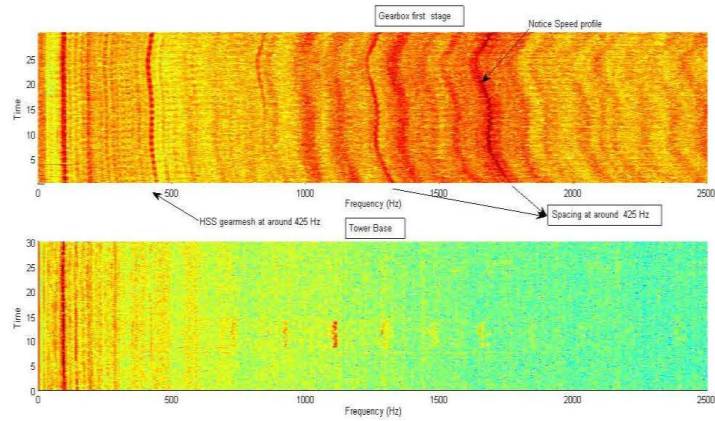


Figure 15 Spectrograms of the gearbox signal (1st stage) and the tower base signal

in Figure 15, GB First Stage; there is a clearer gearmesh frequency compared to GB third stage. This works very well for doing the order tracking compared to the third stage signal.

Figures 16 and 17 show the Generator signals. It is interesting to see the speed profile including strong sideband frequency components spaced at 120 Hz from the 3rd harmonic of the HSS gearmesh. The frequency band between 1000 Hz and 1700 Hz is the one showing these speed variations very clearly in all cases. These sidebands spaced at 120 Hz, but following the varying speed components of the gearbox, are apparently different from the fixed frequency sidebands spaced at 120 Hz described in Report No. 1 (and seen above 2 kHz in Fig. 2), and probably represent genuine vibrations, caused by modulation of the gearmesh forces by the rotating magnetic fields in the stator, as opposed to masking noise from an electrical source. Note that at low speeds, the third sideband almost coincides with the 4th harmonic of gearmesh.

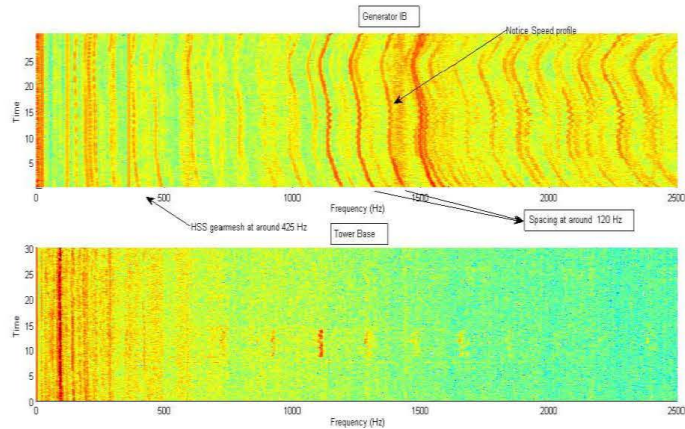


Figure 16 Spectrograms of the generator (inner bearing) and the tower base signal

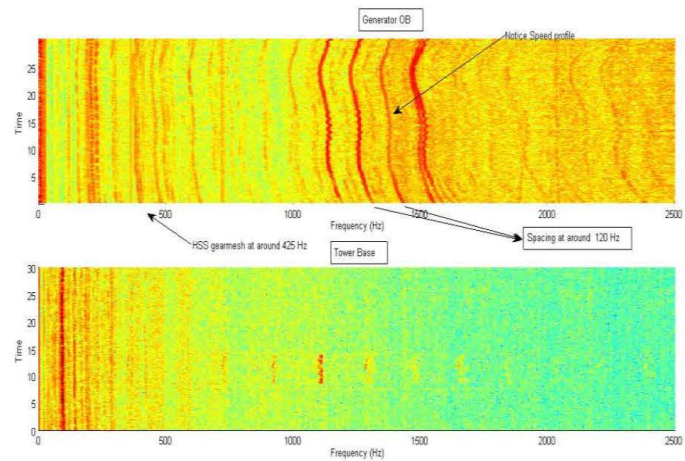


Figure 17 Spectrograms of the generator (outer bearing) and the tower base signal

3. Signal order tracking

The result shown in Figure 18 for order tracking was obtained from the 1st stage gearbox and this was the most successful result obtained after two stages of demodulation to show the harmonics of the 1st gearmesh. The first stage was based around 21 Hz (HSS), while the second was based around 420 Hz (harmonic number 20, guided by initial results). Figure 19 shows the 1st gearmesh frequency before and after the order tracking. The presumed planet pass frequency at 0.8 Hz is seen in sidebands around the gearmesh frequency.

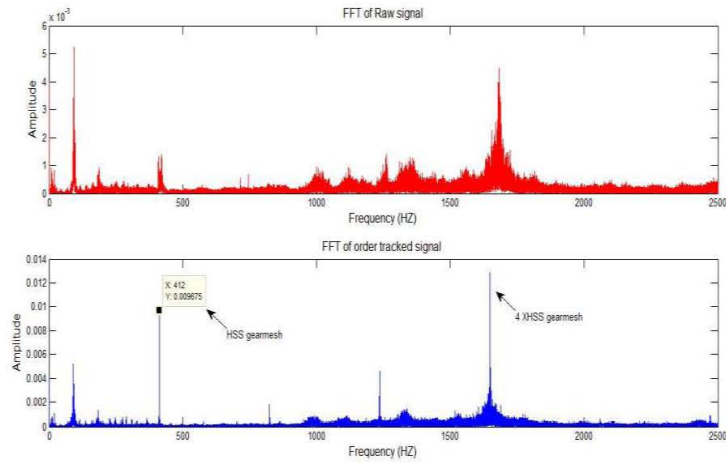


Figure 18 Spectrum of the First stage gearbox. Top: Raw signal. Bottom: after two stages of order tracking

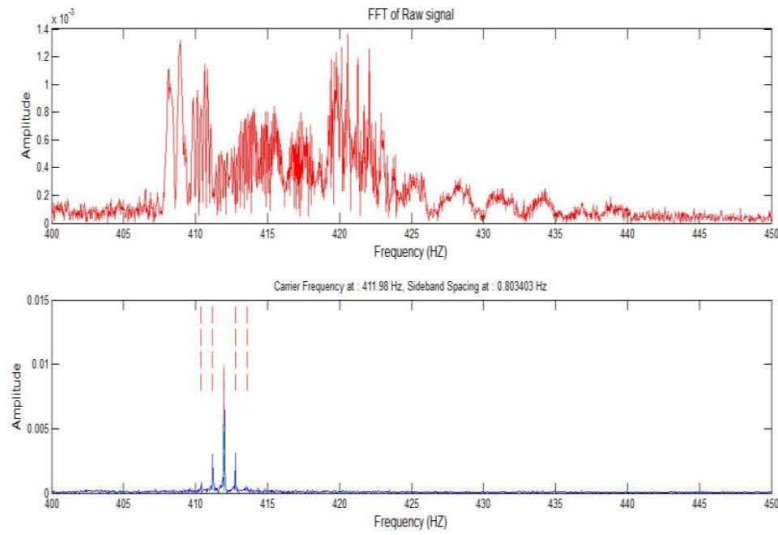


Figure 19 Sidebands around the First gearmesh frequency (most likely at the planet pass frequency)

When order tracking was attempted on the 2nd gearmesh frequency, sidebands at 0.26 Hz (input shaft speed) were noticed around the order-tracked harmonics as can be seen from Figure 20.

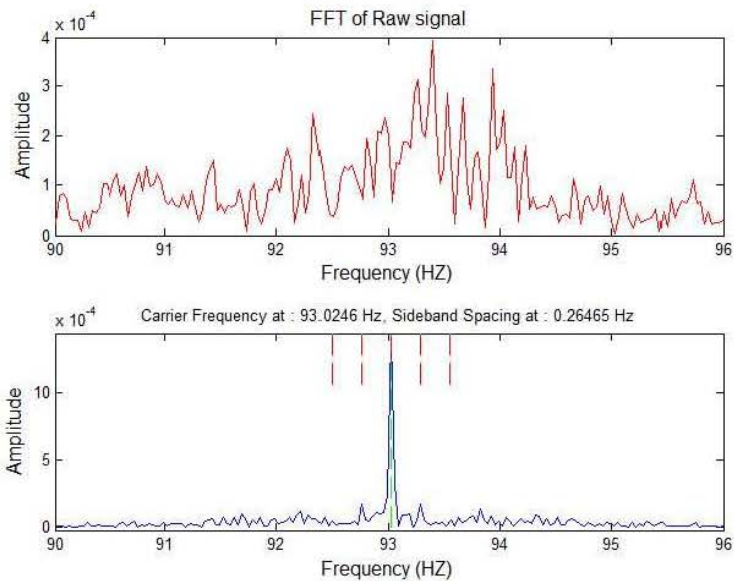


Figure 20 Sidebands around the second gearmesh frequency (most likely at the input frequency)

Conclusion

Analysis of vibrations measured up-tower on the machines in the nacelle was compared with that from measurements made at the base of the tower. The signals were similar only in the low frequency region up to 500 Hz, and were highly attenuated and masked above those frequencies.

For the up-tower measurements, a range of different frequency components could be used to obtain a measure of instantaneous speed and use it to perform order analysis. The best was perhaps the high speed (HS) gearmesh signal and its higher harmonics, in particular the third and fourth, but the generator speed around 21 Hz could also be used (for a first iteration) as could the second gearmesh frequency around 93 Hz. For the measurements at the tower base, the generator shaft speed component and the second gearmesh signal could be used reliably for order tracking, but the HS gearmesh was not present in all signals.

Detailed analysis of the up-tower signals indicated that it should be possible to identify the gears in the transmission, and most of the important frequencies, but there is some doubt as to whether the planetary section has been identified correctly.

Appendix A – Diagnostic Analysis to Identify Gear Parameters

A detailed analysis of one of the signals measured up-tower on the gearbox was made in order to attempt to discover the numbers of teeth on the various gears. The signal measured at the Gearbox 3rd Stage was chosen for this.

First it was desirable to find a section with as little speed variation as possible, and so the whole signal was plotted to find a section with approximately constant RMS value, as this has earlier been seen to correspond to smaller speed variation. First, the signal was decimated by a factor of 8, partly to allow analysis of the longer records (in terms of time) and partly because the information about the various gearmeshes was contained in the valid frequency range to 2500 Hz after downsampling.

Figure A1(a) shows the total signal length, and A2(b) the chosen section of length 600 000 samples.

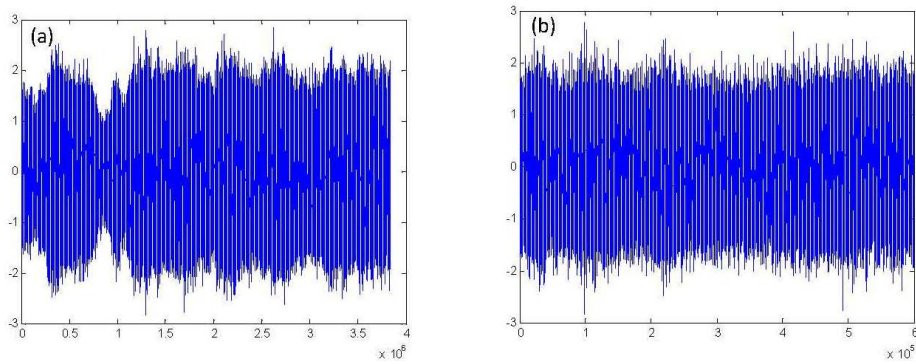


Figure A1 (a) Total record length (b) Section analysed from $1.2-1.8 \times 10^6$ samples

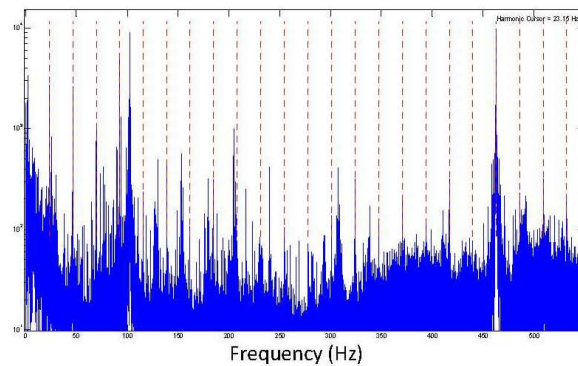


Figure A2 Order tracked spectrum with HSS gearmesh as harmonic No. 20

Figure A2 shows the result of order tracking using the HSS gearmesh as speed reference. The harmonic cursor indicates that the gearmesh frequency is the 20th harmonic of a series most likely corresponding to the generator speed. The mean speed over this record is 23.15 Hz, and inserting that value in the gearmesh spreadsheet gives the values shown in Table A1.

Table A1 Estimated shaft and gearmesh frequencies (for generator mean speed 23.15 Hz)

Estimated Frequencies in the gearbox		
High shaft speed (Hz)		23.15
HS-ST		HS-ST GMF
pinion	20	
gear	113	463.00
Intermediate shaft speed (sun)		4.10
IS-ST		IS-ST GMF
pinion	25	
gear	71	102.43
Low shaft speed (sun)		1.44
Ring gear teeth	105	Epicyclic mesh
Planet gear	39	
Sun gear	27	30.99
Out put speed (carrier)	0.295	
Planet pass frequency	0.885	
Spin frequency	-0.795	

The basis for filling in the rest of the table will now be explained.

Figure A3 is a zoomed spectrum up to 150 Hz, and shows the suspected second gearmesh frequency at around 102.4 Hz. It is seen that even at this level of zoom, the dominant spectrum components are very clear, even in the range below 10 Hz. The first few harmonics of generator speed 23.15 Hz are clear.

The next thing sought was a series of harmonics including both the first and second gearmesh frequencies; these corresponding to the gears mounted on the intermediate shaft.

Figures A4 and A5 are zoom spectra showing two levels of zoom around the HS gearmesh of 102.4 Hz. Figure A4 shows a family of sidebands with a spacing of about 4.1 Hz, and Fig. A5 confirms that this is also a family of harmonics with spacing more accurately 4.097 Hz.

Figure A6 shows that the second gearmesh frequency (102.4 Hz) is the 25th harmonic of the same series.

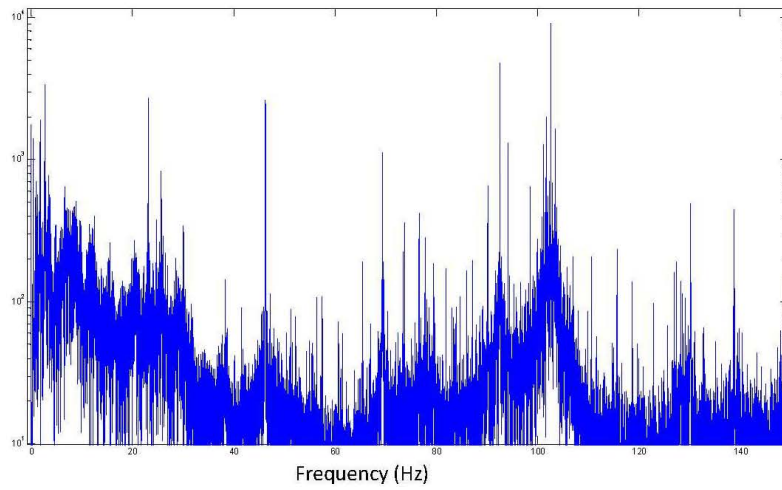


Figure A3 Spectrum zoomed on the frequency range up to 150 Hz

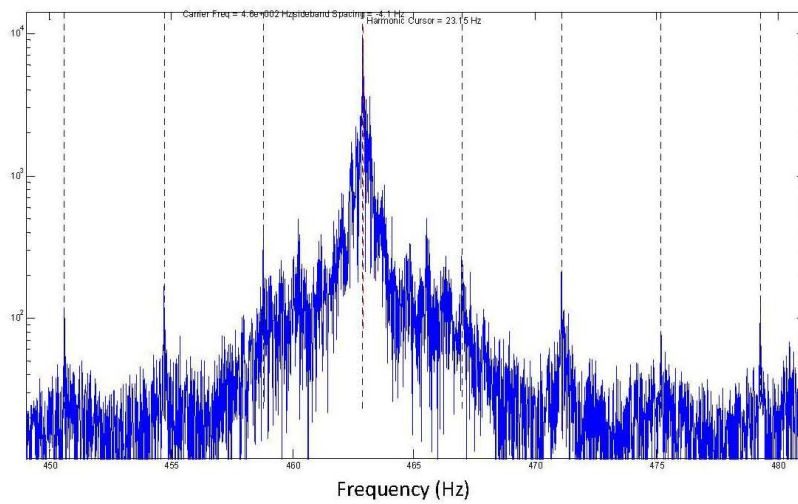


Figure A4 Sidebands around HSS toothmesh with a spacing of 4.1 Hz

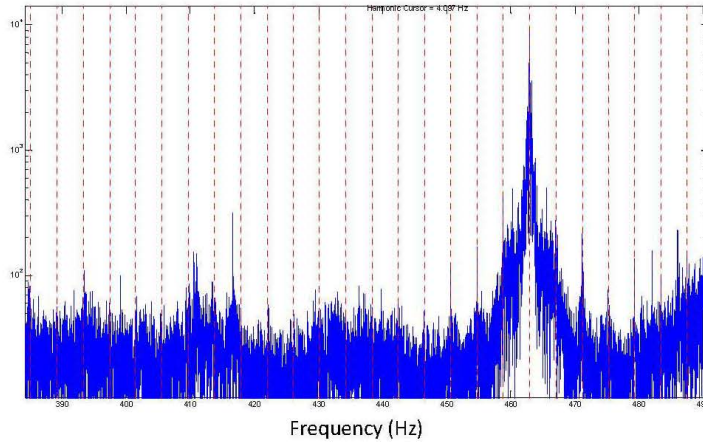


Figure A5 Spectrum showing that the HS gearmesh (462.9 Hz) is the 113th harmonic of a series spaced at 4.097 Hz

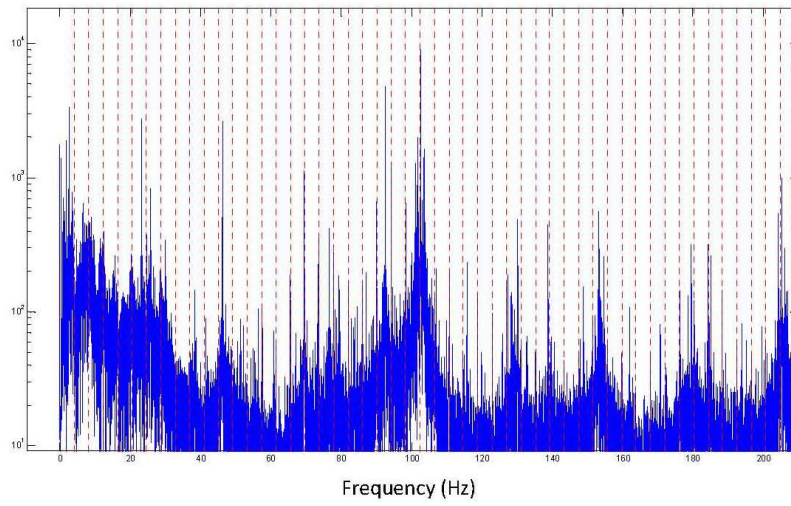


Figure A6 Showing that the second gearmesh frequency is the 25th harmonic of the series spaced at 4.097 Hz.

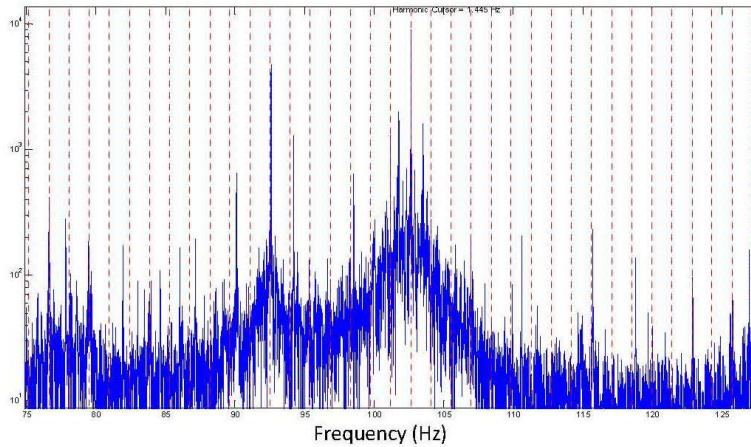


Figure A7 Showing a series of harmonics spaced at 1.445 Hz, which include the second gearmesh frequency (102.45 Hz) as harmonic No. 71

Another series of harmonics is sought for the sun gear shaft, which should also have the second gearmesh frequency (102.4 Hz) as a member. Figure A7 shows that there is a possible series at 1.445 Hz with this gearmesh frequency as harmonic No. 71, and including a number of sidebands around the gearmesh frequency. Note also that there are a pair of strong sidebands spaced at about 0.89 Hz, with others at 1/3 of this spacing. These sideband families are however not subharmonics of the gearmesh frequency, and are suspected to be the input shaft speed (0.29 Hz) and its third harmonic the planet pass frequency (0.89 Hz). It is thus thought that the sun gear speed is 1.445 Hz.

Figures A8 and A9 lend weight to the theory that the input speed is 0.29 Hz, by showing some of the harmonics of a series spaced at 0.8842 Hz (Nos. 28, 29, 30 and 57, 58, 59, respectively). Harmonics 29 and 58 have subharmonics at 1/3 of the spacing as well.

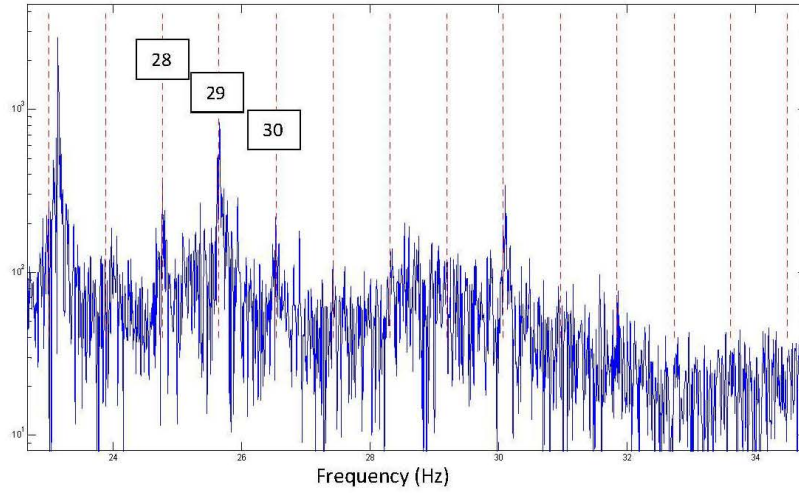


Figure A8 Harmonics of 0.8842 Hz (planet pass frequency) Nos. 28, 29, 30, with the middle one also showing 1/3 spacing (0.29 Hz)

146 Hz

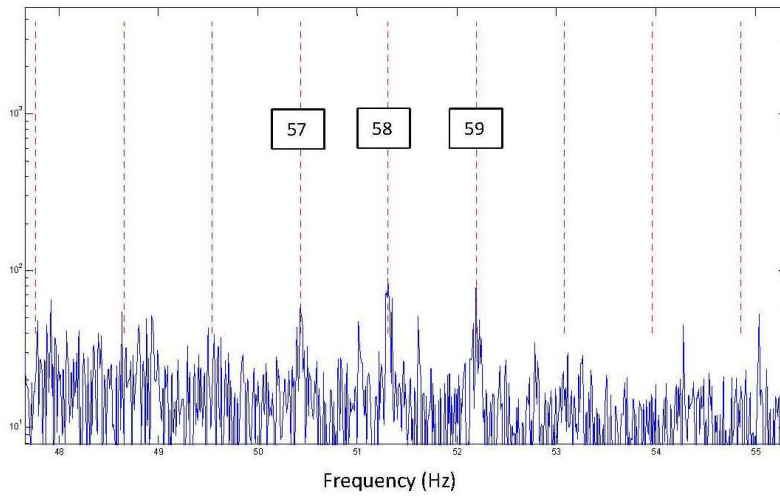


Figure A9 Harmonics of 0.8842 Hz (planet pass frequency) Nos. 57, 58, 59, with the middle one also showing 1/3 spacing (0.29 Hz)

It remains to find the details of the gears in the planetary section. These are subject to considerable restraint, as follows. If S , P , and R are the numbers of teeth on the sun, planet and ring gears, respectively, then in general the following equations should be satisfied:

$$R = S + 2P \quad (1)$$

And either R and S must be both divisible by 3 (simultaneous meshing with all planets) or the sum of R and S must be divisible by 3 (offset meshing of the planets).

By trial and error, the set of gears indicated in Table A1 were arrived at; viz. $R = 105$, $P = 39$ and $S = 27$. These satisfy the rules given above, and also give approximately the right gear ratio. The overall ratio of the gearbox with the parameters in Table A1 is 78.447, whereas the actual is thought to be 78.472. It must be admitted that the hypothetical planetary section is the least likely to be correct, as little evidence could be found to confirm the details. For example, the planetary gearmesh frequency (30.99 Hz in Table A1) could not be located with certainty. Figure A10 shows the harmonics of input speed 0.2942 Hz, including the possible planet gearmesh frequency No. 105, but this is very low. On the other hand, every third harmonic to the left is well represented (some quite strong) and this sometimes occurs with planetary gears (ie the sidebands adjacent to the gearmesh frequency are stronger than the gearmesh itself).

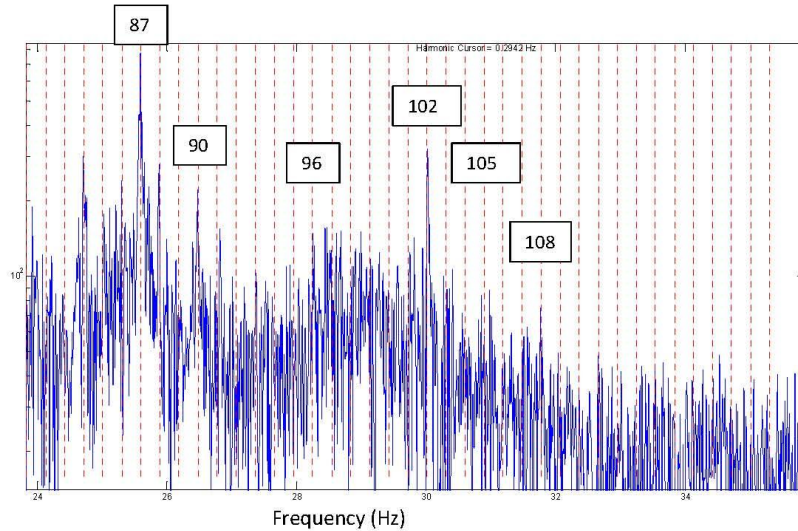


Figure A10 Harmonics of 0.2942 Hz, including planetary gearmesh No.105

APPENDIX C

POSTER AT AWEA WINDPOWER 2012

This poster was prepared by MSI, reviewed and approved by NYSERDA, and submitted to the American Wind Energy Association (AWEA) in April 2012, for presentation at the Association's 2012 Windpower Conference & Exhibition, held June 3–6, in Atlanta, GA. AWEA approved the poster as submitted, and printed it for the conference. The poster was one of 40 in the Performance and Reliability section. Overall approximately 200 posters were on display in a dozen categories ranging from financing to siting to policy. The poster gallery was on the main exhibition floor, and posters were on display from Sunday June 3 through Wednesday June 6. More than 10,000 persons attended Windpower. The poster display included a bin with hard copies and many were picked up by passersby. The MSI Program Manager attended the conference and participated in an hour-long "Meet the Authors" session, where several contacts were made and were being followed up on at the time this report was prepared.

NON-INTRUSIVE PREDICTIVE HEALTH MONITORING FOR WIND TURBINES

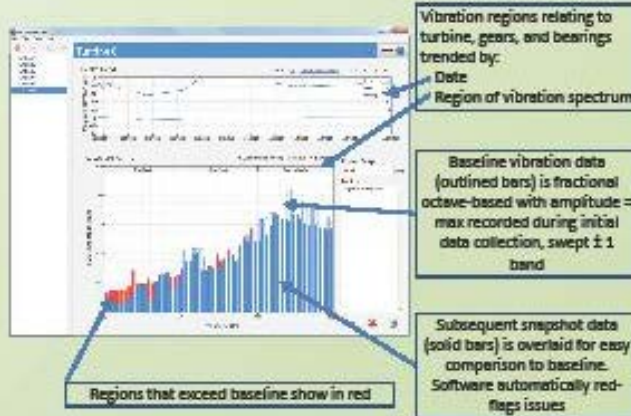
Thomas J. Weber & Jeremy A. Weiss - Mechanical Solutions, Inc. (MSI)

Introduction:

- Nacelle access is inconvenient and can be restricted due to warranty, liability, or business arrangement
- Permanent instrumentation for condition-based maintenance (CBM) or Predictive Maintenance (PdM) is expensive to install and maintain, and requires duplication for each turbine
- A push-button machinery health assessment is needed that uses vibration data collected at the ground level on the exterior of the tower
- MSI is evaluating the merits of tracking machinery health using advanced signal processing techniques applied to vibration data measured at the tower base, with funding from the New York State Energy Research & Development Authority (NYSERDA)
- Questions being answered:
 - Does vibration originating in the nacelle propagate down the tower with enough signal content to make an accurate health assessment?
 - Can advance signal processing techniques harvest quantifiable health information on individual mechanical components from this data?
 - Can this technique be widely applied all turbine makes/models with limited knowledge of mechanical sub-systems?
 - Can this process be automated with the data collection, analysis, and presentation done at the push of a button?

Method:

- A single laptop-powered sensor temporarily attaches by magnet to the tower near ground level
- Software stores and parses vibration data into information relating to turbine, gears, and bearings using a constant percentage bandwidth (CPB) fractional octave spectrum
- Information is trended over time to visualize changes in machinery health
- CPB fractional octave spectrum provides robustness against speed variations



- Initial data measured across a wide speed/load range establishes a baseline after construction, routine maintenance, or major overhaul
- Subsequent 30-second data snapshots are taken weekly, monthly, etc.
- Regions of fractional octave spectrum correspond to vibration sources:
 - < 100 Hz: Turbine and rotors
 - Between 100 and 1,000 Hz: Gears
 - > 1,000 Hz: Bearings
- Snapshots' margin to baseline for each region are trended over time
- User option to apply advanced interactive diagnostics if component information is known (e.g. gear tooth counts, bearing roller dimensions)

Results to Date:

- Field testing and finite element analysis (FEA) confirm that vibration from nacelle-mounted machinery can be measured at the tower base
- Software generated to automate data acquisition, storage, analysis, and presentation
- Seeded rotor, gear, and bearing faults successfully diagnosed in test rig simulating vibration transmission effects from nacelle to tower base

Status and Plans:

- Prototypes are being field tested. Results are promising!
- Seeking Beta testers. Interested? Contact us: tjw@mechsol.com; Barry N. Liebowitz, NYSERDA - bnl@nyserdera.org
- MSI info available at www.mechsol.com

sponsored by
nyserdera
The Energy Research and Development Authority

NYSERDA has not reviewed the information contained herein, and the opinions expressed do not necessarily reflect those of NYSERDA or the State of New York.